

UNCLASSIFIED

AD NUMBER	
AD393555	
CLASSIFICATION CHANGES	
TO:	UNCLASSIFIED
FROM:	CONFIDENTIAL
LIMITATION CHANGES	
TO:	Approved for public release; distribution is unlimited.
FROM:	Distribution authorized to U.S. Gov't. agencies and their contractors; Administrative/Operational Use; OCT 1968. Other requests shall be referred to Air Force Rocket Propulsion Lab., Research and Technology Div., Attn: RPPR/STINFO, Edwards AFB, CA 93523. NOFORN.
AUTHORITY	
AFRPL ltr dtd 17 Jan 1986   AFRPL ltr dtd 17 Jan 1986	

THIS PAGE IS UNCLASSIFIED

AD 393 555-

AUTHORITY:

AFRPL

17 JAN 86



# **SECURITY**

---

## **MARKING**

**The classified or limited status of this report applies to each page, unless otherwise marked.**

**Separate page printouts MUST be marked accordingly.**

---

THIS DOCUMENT CONTAINS INFORMATION AFFECTING THE NATIONAL DEFENSE OF THE UNITED STATES WITHIN THE MEANING OF THE ESPIONAGE LAWS, TITLE 18, U.S.C., SECTIONS 793 AND 794. THE TRANSMISSION OR THE REVELATION OF ITS CONTENTS IN ANY MANNER TO AN UNAUTHORIZED PERSON IS PROHIBITED BY LAW.

NOTICE: When government or other drawings, specifications or other data are used for any purpose other than in connection with a definitely related government procurement operation, the U.S. Government thereby incurs no responsibility, nor any obligation whatsoever; and the fact that the Government may have formulated, furnished, or in any way supplied the said drawings, specifications, or other data is not to be regarded by implication or otherwise as in any manner licensing the holder or any other person or corporation, or conveying any rights or permission to manufacture, use or sell any patented invention that may in any way be related thereto.

AD393555

(UNCLASSIFIED TITLE)  
COMBUSTION TAILORING CRITERIA  
FOR  
SOLID PROPELLANTS

LOCKHEED PROPULSION COMPANY  
REDLANDS, CALIFORNIA

TECHNICAL REPORT AFRPL-TR-68-191

OCTOBER 1968

GROUP - 4  
Downgraded at 3 year intervals;  
declassified after 12 years

10/1/68  
MIL-TR-68-191

SPECIAL HANDLING REQUIRED

NOT RELEASEABLE TO FOREIGN NATIONALS

Foreign National employees of the contractor or subcontractor(s) including those possessing Canadian or United Kingdom reciprocal clearances, are not authorized access to classified information resulting, or used in the performance of this contract unless authorized in writing by the procuring contracting activity.

AIR FORCE ROCKET PROPULSION LABORATORY  
RESEARCH AND TECHNOLOGY DIVISION  
AIR FORCE SYSTEMS COMMAND  
UNITED STATES AIR FORCE  
EDWARDS, CALIFORNIA

**CONFIDENTIAL NOFORN**

(UNCLASSIFIED TITLE)  
COMBUSTION TAILORING CRITERIA  
FOR  
SOLID PROPELLANTS

LOCKHEED PROPULSION COMPANY  
REDLANDS, CALIFORNIA

STANDARD PROPULSION COMPANY

Information to be provided to the Defense Department  
and other Government agencies in accordance with  
the Defense Classification and Declassification  
Guidelines only with prior approval of *AFRPL/PPRC-STD/NOFO*  
*Edwards, Calif. 92523*

GROUP - 4  
Downgraded at 3 year intervals;  
declassified after 12 years

SPECIAL HANDLING REQUIRED

NOT RELEASABLE TO FOREIGN NATIONALS

Foreign National employees of the contractor or subcontractor(s) including those possessing Canadian or United Kingdom reciprocal clearances, are not authorized access to classified information resulting, or used in the performance of this contract unless authorized in writing by the procuring contracting activity.

This document contains information affecting the national defense of the United States, within the meaning of the Espionage Laws, Title 18, U.S.C., Sections 793 and 794. Its transmission or the revelation of its contents in any manner to an unauthorized person is prohibited by law.

CONFIDENTIAL NOFORN

## FOREWORD

This is the fourth phase report issued under Contract F04611-67-C-0089. Reported herein is research conducted between 1 July and 1 October 1968. The report was prepared by R. L. Derr and M. W. Beckstead, Engineering Research Department, Lockheed Propulsion Company (LPC). Contributors to this program include N. S. Cohen, L. Asaoka, R. L. Coates, W. R. Glace, C. F. Price, L. L. Stiles, and W. West, all representing Lockheed Propulsion Company.

Acknowledgement is given to Naval Weapons Center, China Lake, California and Mr. Thom Boggs of NWC for help in obtaining and interpreting scanning electron microscope photographs of extinguished propellant samples.

Work performed under this contract is monitored by the Air Force Rocket Propulsion Laboratory (AFRPL), Edwards, California. The Project Officer is Captain Charles E. Payne, AFRPL/RPMCP.

This report is classified CONFIDENTIAL-NOFORN because it makes reference to advanced propellant formulations and ingredients of interest to the Air Force.

Publication of this report does not constitute Air Force approval of the findings or conclusions. It is published only for the exchange and stimulation of ideas.

Captain C. E. Payne  
AFRPL/RPMCP

## ABSTRACT

The objective of this research program is to develop an analytical model describing the steady-state combustion of solid propellants which is suitably equipped to provide combustion tailoring criteria for both state-of-the-art and advanced propellant formulations. The model will be developed and implemented from experimental data acquired from a dual experimental program. Tests with small samples of propellants will provide experimental data for modeling the propellant combustion process for different ingredient variations, e. g., oxidizer size, concentration, and metals. Additional tests in apparatus simulating the environment of a rocket motor will provide experimental data showing the effect of rocket motor environment upon the combustion process. During Phase IV, analytical work was directed towards modeling the gaseous reaction zones above the surface of an ammonium perchlorate oxidized propellant. Experimental work was directed towards testing a series of propellants containing four different oxidizers.

(The reverse is blank)

## CONTENTS

<u>Section</u>	
	<u>Page</u>
I      INTRODUCTION	1
II     PROGRAM SUMMARY	3
1. ANALYTICAL PROGRAM	3
2. EXPERIMENTAL PROGRAM	3
a. Formulations and Burning Rates of Propellants Tested	3
b. Surface Structure Studies of Extinguished Samples	3
c. Thermal Profile Studies of Solid Propellants	4
III    ANALYTICAL INVESTIGATION	5
1. GENERAL DISCUSSION	5
2. THE TWO-STAGE FLAME	6
IV    EXPERIMENTAL INVESTIGATION	15
1. GENERAL DISCUSSION	15
2. PROPELLANT FORMULATIONS AND BURNING RATES	16
a. Approach	16
b. Propellants Containing AP	16
c. Propellants Containing KP	21
d. Propellants Containing HAP	24
e. Propellants Containing HMX	26
3. STUDY OF THE SURFACE STRUCTURE OF EXTINGUISHED PROPELLANTS	26
4. THERMAL PROFILE STUDIES USING MICROTHERMOCOUPLES	37

## CONTENTS (Continued)

<u>Section</u>		<u>Page</u>
V	PLANS FOR THE NEXT PHASE	43
1.	ANALYTICAL INVESTIGATION	43
2.	EXPERIMENTAL INVESTIGATION	43
NOMENCLATURE		45
REFERENCES		47

## ILLUSTRATIONS

<u>Figure</u>		
	<u>Page</u>	
1 Proposed Flame Structure	7	
2 Model of Proposed Flame Structure	9	
3 Burning Characteristics of Propellants Showing Effect of AP Level	18	
4 Burning Characteristics of Propellants Showing Effect of AP Size	20	
5 Burning Characteristics of Propellants Showing Effect of KP Level	22	
6 Burning Characteristics of Propellants Showing Effect of KP Size	23	
7 Burning Characteristics of Propellants Showing Effect of HAP Size	25	
8 Burning Characteristics of Propellants Showing Effect of HMX Level	27	
9 Burning Characteristics of Propellants Showing Effect of HMX Size	28	
10 SEM Photographs of 835-2-2 at 100 psi	30	
11 SEM Photographs of 835-2-2 at 200 and 300 psi	31	
12 SEM Photographs of 835-2-4 at 100 and 800 psi	33	
13 SEM Photographs of 835-2-4 at 600 psi	34	
14 SEM Photographs of 835-2-4 at 600 psi Showing Crystal Detail	35	
15 SEM Photographs of Mod AGC-NOAL at 600 psi	36	
16 SEM Photographs of Mod AGC-NOAL at 528 psi	38	
17 Thermal Profile of 835-6-4 at 200 psia	39	
18 Thermal Profile of 835-6-4 at 300 psia	40	
19 Thermal Profile of 835-6-4 at 400 psia	41	

(The reverse is blank)

## SECTION 1

## INTRODUCTION

Past studies of solid propellant combustion have been directed toward both experimental and analytical investigations of the combustion process. Experimental studies have provided a wealth of information pertaining to steady-state and nonsteady-state combustion for a variety of propellants and propellant ingredients. Analytical studies have been directed toward a variety of propellant systems. However, these studies have not been successful in representing the combustion process successfully such that they can account for changes in oxidizer, binder, catalysts, and metal additives in the framework of establishing combustion tailoring criteria for a given propellant system.

In April 1967, the Air Force Rocket Propulsion Laboratory (AFRPL) contracted Lockheed Propulsion Company (LPC) to study the combustion of solid propellants with the objective of providing such criteria. The program includes a comprehensive combustion literature survey to establish the present state of combustion knowledge and provide a baseline for analytical and experimental work (3).

In the first year, the program included the design and fabrication of combustion research apparatus, representative of a motor and amenable to instrumental monitoring of various facets of steady-state and transient combustion. Tests with a series of well-characterized propellants also were conducted in the first year effort to check out experimental apparatus.

In the second year, a series of state-of-the-art propellants and propellants containing advanced ingredients are being tested to provide data which will be used to develop and implement an analytical model of the combustion process. Development will progress from a model capable of describing the burning rate characteristics of simple propellant systems, i. e., non-metalized and uncatalyzed, to one that is capable of describing the burning rate characteristics of more advanced propellant systems, i. e., propellants containing metal additives and energetic binders. In that way, the capability of combustion tailoring will be built into the analytical model.

The two-year combustion research program can be divided into five major tasks summarized as follows:

- (1) Literature survey
- (2) Design, fabrication, and pretest check of combustion research apparatus
- (3) Experimental program with well-characterized propellants

- (4) Experimental program with operational and advanced formulations
- (5) Analysis and formulation of combustion tailoring model

At the present, Parts 1, 2 and 3 are completed. Results contained herein cover research conducted during the second quarter of the second-year effort.

## PROGRAM SUMMARY

This report describes work accomplished on a study of the combustion of solid propellants. The overall goal of the program is to develop an analytical model suitably equipped to provide combustion tailoring criteria both state-of-the-art and advanced propellant formulations. The model will be developed and implemented from data acquired from an experimental program. Accomplishments during the report period are summarized in the following subsections.

## 1. ANALYTICAL PROGRAM

Utilizing the model as described in the previous report, the energy release in the flame zone was determined to be of critical importance in the model. Therefore, a more realistic description of the flame zone has been incorporated into the model. The new description is a two-stage flame consisting of a laminar, premixed flame describing the AP combustion followed by a diffusion flame in which the reactants are the oxidizing products from the AP flame and the fuel-rich products from the binder pyrolysis. The two-stage flame has been described in terms of one-dimensional heat transfer equations. The flame stand-off distances for the two flames are approximated by employing the kinetics for a second order reaction for the premixed flame and by averaging the results of two-dimensional diffusion equations for the diffusion flame.

## 2. EXPERIMENTAL PROGRAM

## a. Formulations and Burning Rates of Propellants Tested

A series of propellants containing four different oxidizers were tested. Burning characteristics of these propellants are reported in terms of measured burning rate and self-extinguishment as a function of oxidizer load and concentration.

## b. Surface Structure Studies of Extinguished Samples

Scanning electron microscope photographs are presented showing the extinguished surface of a non-metallized ammonium perchlorate propellant burned over a pressure range of 100 to 600 psia. The surface structure of the burning propellant is inferred through analysis of these photographs. Results show that ammonium perchlorate crystals protrude above the binder surface at low pressure and are below this surface at high pressures. In addition, propellants having a polyurethane binder show a melt on the surface whereas those using a CTPB binder show no evidence of melt.

BEST  
AVAILABLE COPY

c. Thermal Profile Studies of Solid Propellants

Thermal profiles measured with microthermocouples are presented for a non-metalized propellant containing HMX. The surface temperature was found to be about  $780^{\circ}\text{C}$  for this propellant at pressures of 200, 300, and 400 psia. Differential scanning calorimeter results are presented for comparison to the shape of the thermal profile.

### SECTION III

#### ANALYTICAL INVESTIGATION

##### 1. GENERAL DISCUSSION

The basic philosophy that is being followed in developing the combustion tailoring model (CT model) is similar to that employed by Hermance (1, 2) and has been discussed in some detail in the previous reports (3, 4, 5). In the last report, the geometrical structure of the propellant surface was mathematically modeled assuming that the oxidizer surface is spherical, but always joining the fuel at the fuel surface. Based on this assumption, equations were derived (Equations 17, 18 and 19, Reference 5) describing the amount of propellant surface area undergoing reaction by oxidizer decomposition, fuel pyrolysis, or heterogeneous reaction. These equations were then incorporated into the basic equation of the model which is (5 or 1)

$$r = \frac{1}{\rho_p} \left[ m_b \left( \frac{S_b}{S_o} \right) + m_{ox} \left( \frac{S_{ox}}{S_o} \right) + m_{hr} \left( \frac{S_{hr}}{S_o} \right) \right] \quad (1)$$

where  $m$  represents the mass flux,  $S$  the surface area and the subscripts stand for fuel, oxidizer and surface reactions (see the Nomenclature for a definition of all terms). The mass flux terms are evaluated utilizing Arrhenius expressions of the form

$$m_i = \rho_i A_i \exp(-E_i/RT_s) \quad (2)$$

(see Equations 20, 21 and 22, Reference 5). Thus, it can be seen that the burning rate of the propellant can be calculated as a function of the surface temperature and the several parameters that are involved.

Using the same gas phase analysis and heat transfer mechanism as Hermance to determine the surface temperature, and using what appeared to be reasonable parameter values, the burning rate was calculated for a typical composite propellant. This resulted in burning rates that were at least an order of magnitude greater than the experimental data; the problem being that the calculated surface temperature was unreasonably high. Application of the LPC optimization program (optimizing on five parameters at a time) indicated that the value of the heat release associated with the ammonium perchlorate gas phase decomposition would have to be unreasonably low in order to give realistic surface temperatures and burning rates. Examining these results in detail and referring to the basic equations, it was concluded that a more realistic flame structure must be used than that of Hermance. In the Hermance model, the heat release due to the AP flame was included in the summation of the surface heat release which in turn was employed as a boundary condition for the differential equations describing the heat transfer from the propellant flame. This was an admitted assumption, but appeared

to be within reason (1, 2). However, within the framework of the present model with emphasis on the oxidizer decomposition, it appears that the AP flame must not be included in the surface processes. Including it tends to force the surface temperature to that of the AP flame temperature, which is obviously incorrect.

## 2. THE TWO-STAGE FLAME

The results of the model as described above have led to the conclusion that the heat release in the flame must be described as occurring in two discrete steps. Actually, this describes the flame zone more accurately than does the assumption that there is a single release of energy at a certain distance from the propellant surface. The following is a description of the composite propellant flame structure as envisioned by the authors.

It is assumed that the ammonium perchlorate (AP) decomposes into ammonia and perchloric acid (6). The thin layer of molten AP which apparently covers the crystal surface (see Section IV and Reference 7) will be assumed to occur in a narrow enough zone that it can be ascribed to the surface itself. (As a greater understanding of this characteristic and its effect on combustion is arrived at, perhaps a more accurate mathematical description can be achieved.) The ammonia and perchloric acid then react in the gas phase and burn essentially as a mono-propellant flame at or near the adiabatic flame temperature of AP. The equilibrium products of this flame, mainly  $\text{HCl}$ ,  $\text{H}_2\text{O}$ ,  $\text{N}_2$  and  $\text{O}_2$ , then flow from the AP flame to where these and possibly other minor oxidizing species react with the decomposition products from the fuel in a diffusion flame.

The fuel binder initially undergoes pyrolysis at a temperature close to that of the AP, liberating methane, free carbon, hydrogen, and other products, the exact species and concentration being determined by the composition of the binder. The free carbon and either methane or hydrogen are the principal fuel species that react with the oxidizers in the diffusion flame. This can be determined from comparing the thermochemical calculations for a propellant with calculations for AP alone and binder pyrolysis alone but in the proper proportions to simulate the given propellant.

The effect of pressure on this postulated flame structure is described schematically in Figure 1. At low pressures the AP flame will be extended from the surface, acting as a premixed flame, and the diffusion flame will be close to the AP flame, diffusion being enhanced by the low pressure. At higher pressures, the AP flame moves closer to the surface while diffusion is restricted causing the second flame to be extended considerably from the surface. This would indicate that at the higher pressures, the AP dominates the combustion while at lower pressures the effect of the binder plays a more important part, which is in keeping with actual observations. At low pressures, as the AP flame stand-off distance is increased the possibility of the perchloric

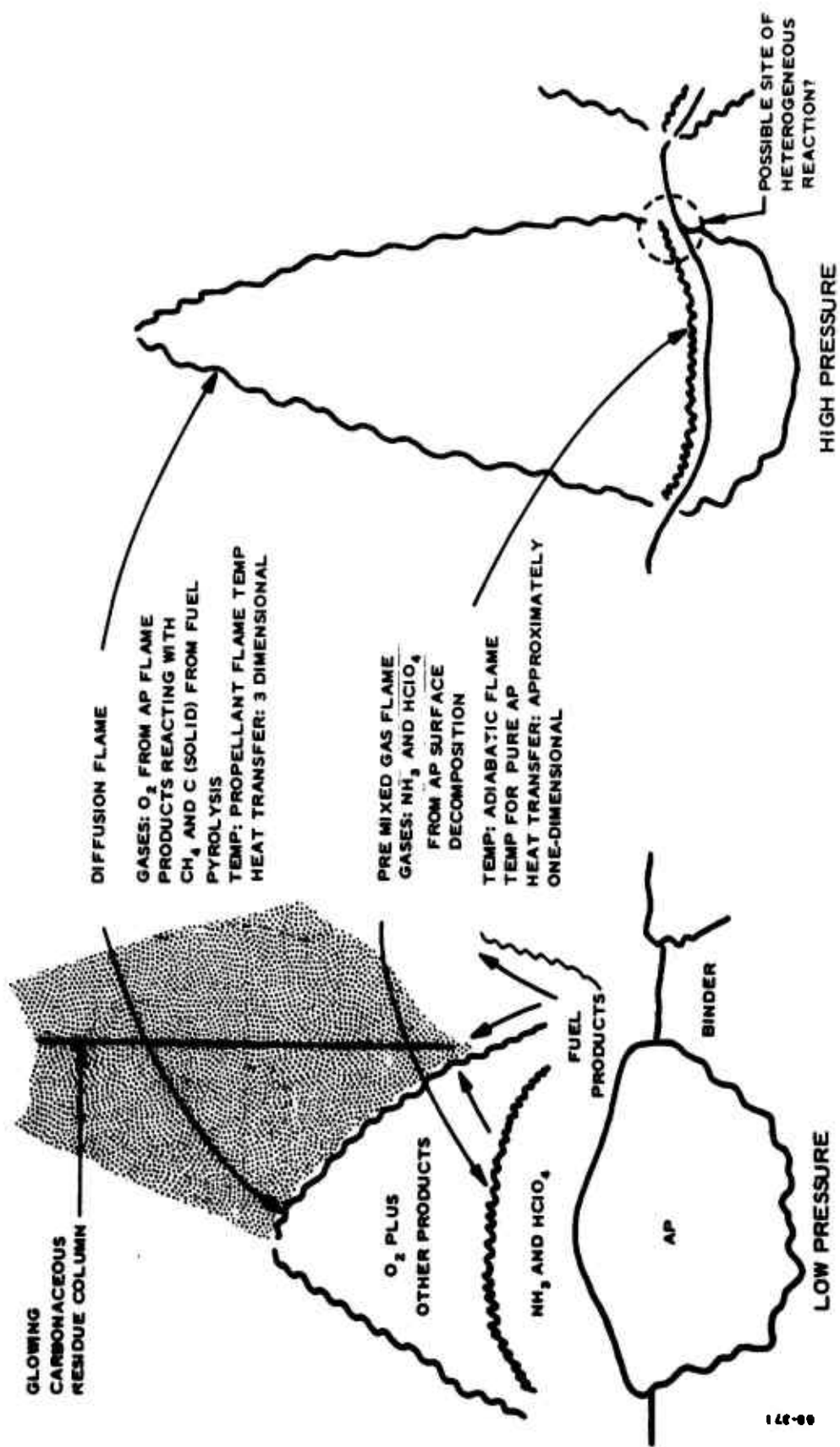


Figure 1 Proposed Flame Structure

acid diffusing into the fuel stream is greatly enhanced. This could result in heterogeneous reactions between the acid and the binder or gas phase reactions with the pyrolysis products. At high pressure, the AP fuel geometric set-up may possibly have some heterogeneous attack. In either case a separate heat source must be considered.

It is impossible to describe the above flame structure in tractable mathematical expressions without making several simplifying assumptions. Figure 2 contains the model of the proposed flame structure with brief notations as to the assumptions leading to the calculation of the surface temperature. As was pointed out in the previous subsection, the surface temperature must be determined in order to solve Equations (1) and (2). This is done by assuming that the heat transfer from the gas phase to the solid surface is approximately one-dimensional. For the AP flame this is probably a reasonable assumption, but the diffusion flame is obviously not one-dimensional. The assumption that it is one-dimensional is only justified by the reasoning that at most pressures, the heat transfer from the diffusion flame is small compared to that of the oxidizer decomposition flame, and that some assumption is necessary in order to arrive at a tractable mathematical problem. The stand-off distance for the diffusion flame is determined from the two-dimensional analysis of Burke and Schumann (8) which should add to the validity of the assumption.

In the analysis that follows the surface temperature that is calculated is the surface temperature of the AP. It will then be assumed that the surface temperature of the binder is essentially the same as that of the AP. In the framework of the present model (and on a physical basis) this appears to be a reasonable assumption considering that the AP is the dominant ingredient of the propellant. Also, the results of the thermocouple measurements (see Section IV) seem to indicate that the measured temperature, which is necessarily in the binder, varies considerably with different oxidizers indicating that the surface temperature is closely related to that of the oxidizer. Thus, assuming that the two temperatures are equivalent seems reasonable.

The mathematical formulation of the flame structure follows. The energy equation in one-dimension for steady state conditions and constant thermal properties is:

$$\alpha_t \frac{d^2T}{dx^2} - r \frac{dT}{dx} + Q' \exp(-E/RT_s) = 0 \quad (3)$$

If it is assumed that the heat releases take place at the boundaries only, Equation (3) becomes

$$\alpha_t \frac{d^2T}{dx^2} - r \frac{dT}{dx} = 0 \quad (4)$$

with the general solution being

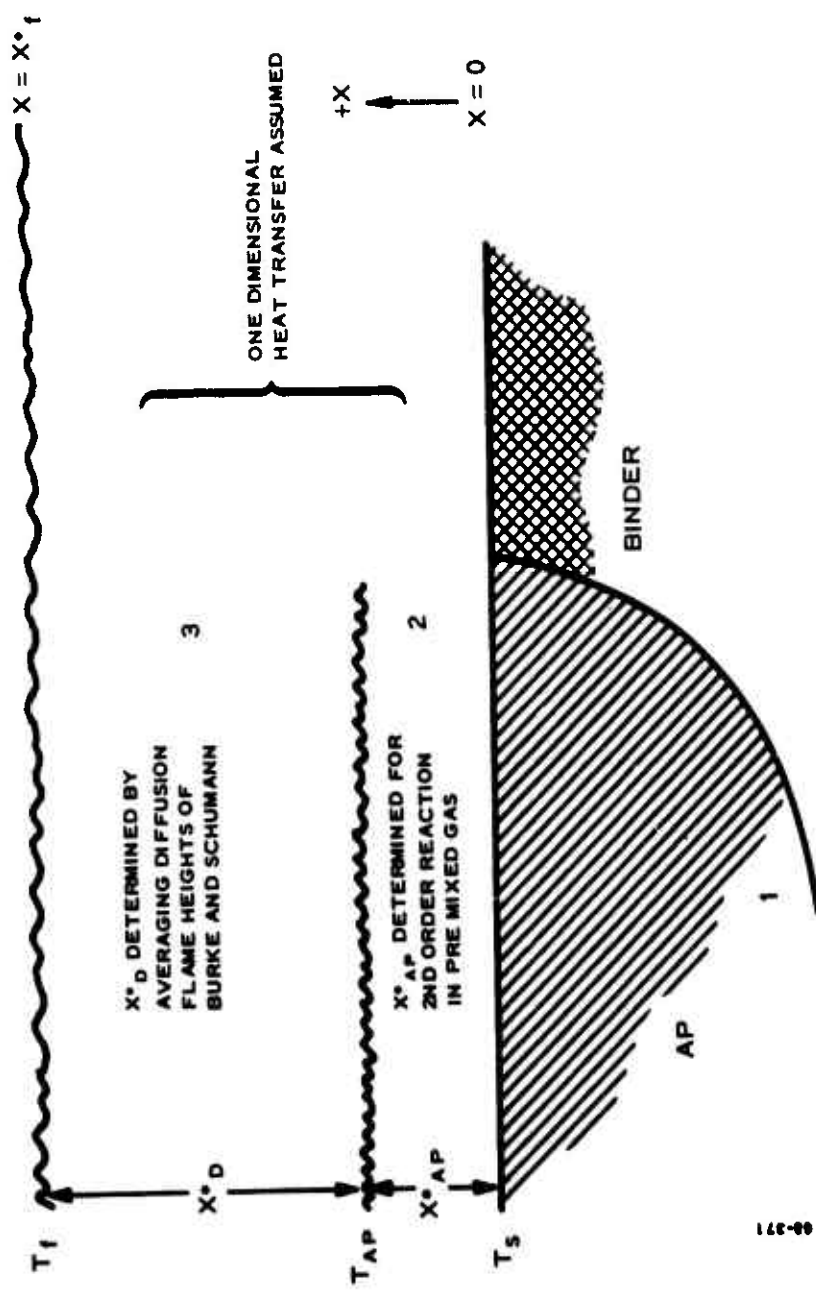


Figure 2 Model of Proposed Flame Structure

$$T = A + B \exp(rx/\alpha_t) \quad (5)$$

The derivative with respect to distance is

$$\frac{dT}{dx} = \frac{r}{\alpha_t} B \exp(rx/\alpha_t) = \frac{r}{\alpha_t} B \exp(\xi) \quad (6)$$

where  $\xi$  is a non-dimensional distance. The boundary conditions are

$$\text{at } x = -\infty, \quad T = T_0$$

$$\text{at } x = 0, \quad T = T_s$$

$$-\lambda_1 \frac{dT_1}{dx} + m_T c_1 T_1 - m_T Q_L = -\lambda_2 \frac{dT_2}{dx} + m_T c_2 T_2 \quad (7)$$

$$\text{at } x = x_{AP}^*, \quad T = T_{AP}$$

$$-\lambda_2 \frac{dT_2}{dx} + m_T c_2 T_2 + m_T Q_{AP} = -\lambda_3 \frac{dT_3}{dx} + m_T c_3 T_3$$

$$\text{at } x = x_f^*, \quad T = T_f$$

$$-\lambda_3 \frac{dT_3}{dx} + m_T c_3 T_3 + m_T Q_f = -\lambda_4 \frac{dT_4}{dx} + m_T c_4 T_4$$

$$\text{at } x > x_f^*, \quad \frac{dT_4}{dx} = 0$$

The heat releases thus written represent an endothermic reaction at the surface and two exothermic reactions in the gas phase. Combining the last two boundary conditions and assuming that the thermal properties are constant across the flame front

$$-\lambda_3 \frac{dT_3}{dx} = -m_T Q_f \quad (8)$$

Equation (6) for zone 3 becomes

$$\frac{dT_3}{dx} = \frac{r}{\alpha_{t_3}} \frac{T_f - T_{AP}}{\exp(\xi_f^*) - \exp(\xi_{AP}^*)} \exp(\xi_3^*) \quad (9)$$

Combining Equations (8) and (9) at  $x = x_f^*$  gives

$$T_f - T_{AP} = \frac{Q_f}{C_g} \left[ 1 - \exp(-\xi_D^*) \right] \quad (10)$$

$$\text{where } \xi_D^* = \xi_f^* - \xi_{AP}^*$$

At the AP flame, assuming constant thermal properties, the boundary condition reduces to

$$-\lambda_g \frac{dT_2}{dx} + m_T Q_{AP} = -\lambda_g \frac{dT_3}{dx} \quad (11)$$

Equation (6) for zone 2 becomes

$$\frac{dT_2}{dx} = \frac{r}{\alpha_g} \frac{T_{AP} - T_s}{\exp(\xi_{AP}^*) - 1} \exp(\xi) \quad (12)$$

Combining Equations (9), (11) and (12) yields

$$T_{AP} - T_s = \left[ \frac{Q_{AP}}{c_g} + \frac{T_f - T_{AP}}{\exp(\xi_D^*) - 1} \right] \left[ 1 - \exp(-\xi_{AP}^*) \right] \quad (13)$$

In zone 1 for the solid AP, Equation (6) becomes

$$\frac{dT_1}{dx} = \frac{r}{\alpha_{t_1}} (T_s - T_o) \exp(\xi) \quad (14)$$

Combining Equations (12) and (14) with the surface boundary conditions (i. e.  $x = 0$ )

$$-m_T c_g (T_s - T_o) + m_T c_g T_s - m_T Q_L = \frac{-m_T c_g (T_{AP} - T_s)}{\exp(\xi_{AP}^*) - 1} + m_T c_g T_s \quad (15)$$

and thus

$$T_s = \frac{c_1}{c_g} T_o - \frac{Q_L}{c_g} + \frac{T_{AP} - T_s}{\exp(\xi_{AP}^*) - 1} \quad (16)$$

Incorporating Equations (10) and (13) into Equation (16) gives the surface temperature as

$$T_s = \frac{c_1}{c_g} T_o - \frac{Q_L}{c_g} + \frac{Q_{AP}}{c_g} \exp(-\xi_{AP}^*) + \frac{Q_f}{c_g} \exp(-\xi_f^*) \quad (17)$$

Combining Equation (17) with Equations (1) and (2) results in a transcendental equation in the burning rate due to the exponentials in  $\xi$ .

The flame stand-off distances must be evaluated in order to solve Equation (17). The AP flame has been assumed to be a premixed flame and it would appear reasonable to assume that it is controlled by a second order reaction. Thus, the stand-off distance is the product of the average gas velocity and the average reaction time,  $x^* = v_g \tau$ . Where

$$v_g = \frac{m_{ox}}{\rho_g A_{AP}} \text{ and } \tau = \frac{1}{\rho_g A_{AP} A_{AP} \exp\left(-\frac{E_{AP}}{RT_{AP}}\right)} \quad (18)$$

or

$$x_{AP}^* = \frac{m_{ox}}{A_{AP} \exp\left(-\frac{E_{AP}}{RT_{AP}}\right)} \left(\frac{RT_{AP}}{PM}\right)^2 \quad (19)$$

The diffusional stand-off distance is approximated utilizing the analysis of Burke and Schumann (8). They determined the total height (i. e., at the center of the crystal in Figure 1) of diffusional flames as a function of the surface dimensions. Averaging this flame height in order to simulate the one-dimensional model gives

$$\frac{x^*}{D} = \eta_{av} \frac{vb^2}{D} \quad (20)$$

where  $b$  is a dimension of the system. The mass diffusivity of gases are pressure and temperature dependent as is the velocity. Thus,

$$\frac{v}{D} = \frac{m_{ox} RT}{PM D_o} \frac{P}{T^v} = \frac{m_{ox} (R/M)}{D_o T^{0.75}} \quad (21)$$

Where  $v$  has been taken as approximately 1.75 (9). Therefore the diffusional distance can be calculated as a function of the regression rate, the average gas temperature, a parameter relating to the oxidizer particle size and weight fraction (i. e.  $b$ ), and an averaged non-dimensional height which is also a function of  $b$ .

The heat releases for the AP can be readily evaluated. The  $Q_L$  can be taken as the endothermic heat of sublimation that has been reported (6, 10). The gas phase heat release can be calculated from the flame temperature assuming an average heat capacity. This leaves the heat release at the diffusion flame front to be evaluated. This can be done in the same way as  $Q_{AP}$  is evaluated. Assuming a mean average heat capacity for the solid propellant and the combustion gases, the sum of the various heat releases multiplied by the appropriate weight factor is equal to the sensible heat.

$$\bar{c} (T_f - T_o) = \alpha (-Q_c) + (1-\alpha)(-\Delta H_p) + \alpha Q_{AP} + Q_f$$

$$Q_f = \bar{c} (T_f - T_o) - \alpha (Q_{AP} - Q_L) + (1-\alpha) \Delta H_p$$

or

$$Q_f = \bar{c} (T_f - T_o) - \alpha \bar{c} (T_{AP} - T_o) + (1-\alpha) \Delta H_p \quad (22)$$

Thus, the heat release for the flame includes the effect of the binder, and this effect becomes most predominant at low pressures.

With this method of determining the surface temperature, Equation (1) can now be solved for the linear burning rate of the propellant.

(The reverse is blank)

**CONFIDENTIAL**  
(This page Unclassified)**SECTION IV**  
**EXPERIMENTAL INVESTIGATION****(U) 1. GENERAL DISCUSSION**

The objective of the experimental studies conducted in this research program is to supply information regarding the combustion process of selected propellant systems necessary for the development of the CT model. A great deal of experimental data are available in the literature for this purpose and have been compiled in the literature survey (3). However, in many cases, these data are incomplete for the purposes of developing a CT model for specific propellant systems. As a result, a two-part experimental program is being conducted to obtain these data. The first part supplies insight into the physical processes occurring during the combustion of solid propellants. Tests are conducted in windowed apparatus using small samples of propellants.

These tests yield the following data:

- Burning rate characteristics of propellants as measured in a combustion bomb environment
- High speed cinematography studies of burning propellant surfaces, including metal activity
- Surface structure studies through examination of extinguished surfaces with photomicrographic techniques
- Thermal wave profile studies through the use of a micro-thermocouples embedded in the propellant

The second part deals with the effect of a motor environment upon the combustion characteristics of solid propellants. These tests are conducted in a windowed slab combustor (4 and 5), closely representing the environment of a rocket motor. This combustor uses two opposed propellant slabs of 6.0 by 2.0 by 0.625 inch dimensions.

Data from these tests include:

- Burning rate characteristics of propellants are measured in a rocket motor environment
- Heat flux levels generated by the burning propellant in this environment
- Metal combustion efficiencies, in terms of percent unburned metals issuing from the slab combustor nozzle and c\* efficiency

**CONFIDENTIAL**

Data from tests conducted in the slab combustor are not used directly in the development of the analytical model. Rather, these tests provide data that can be used as boundary conditions in the CT model representing the effect of the motor environment upon the combustion process (e. g., heat flux from the thermal environment and the influence of metal combustion on the environment).

In the following, results from experiments conducted in the past report period are presented and discussed in terms of the CT model development.

## 2. PROPELLANT FORMULATIONS AND BURNING RATES

### a. Approach

(C) In the last phase report (5), a list of propellants was presented comprised of propellant systems containing different ingredients deemed important for experimental study. The list consisted of two parts. The first considered propellants containing oxidizers of various type (viz. AP, KP, HAP, and HMX), concentration, and grind sizes. These propellants are used in experiments to gain insight into the physical processes occurring during combustion. Formulation for these propellants are summarized in Table I.

(C) The second part of the list considered propellants containing metal (viz. aluminum and LMH-1) and active binders (NF binders). These propellants also are tested to gain insight into the physical processes occurring during combustion. However, additional tests will be conducted in the slab combustor using the metalized propellants and selected non-metalized propellants for control purposes.

(C) A polyester binder with isocyanate cure was used for the binder in each of the propellants except the formulation containing HAP. For that propellant, a saturated binder (hydroxyl-terminated hydrogenated polybutadiene) was used because of compatibility problems between the binder and the HAP. These binders will be referred to as polyurethane (PU)-type and saturated hydrocarbon binders in the following discussions.

### b. Propellants Containing AP

(U) Five different formulations were prepared using AP in three unimodal particle distributions (viz. 8, 50, and 200-micron mean diameter) and three concentrations (viz. 70, 74, and 78 percent by weight). Formulations using the fine and coarse grinds contained 74-percent AP while the medium grind was used in formulations containing the three AP concentrations. The maximum solids loading of 78 percent by weight was determined by adding 50-micron AP to an uncured mix until a viscosity was attained which allowed satisfactory cast properties.

(U) Burning rates for three propellants having the same oxidizer grind size (50 microns) and changes in the AP concentration are presented in Figure 3. It can be seen that increasing the concentration of AP in this

**CONFIDENTIAL**

TABLE I  
FORMULATIONS FOR PROPELLANTS CONTAINING DIFFERENT OXIDIZERS  
PROPELLANT CODE NUMBER (835-)

**CONFIDENTIAL**

CONFIDENTIAL

(This page Unclassified)

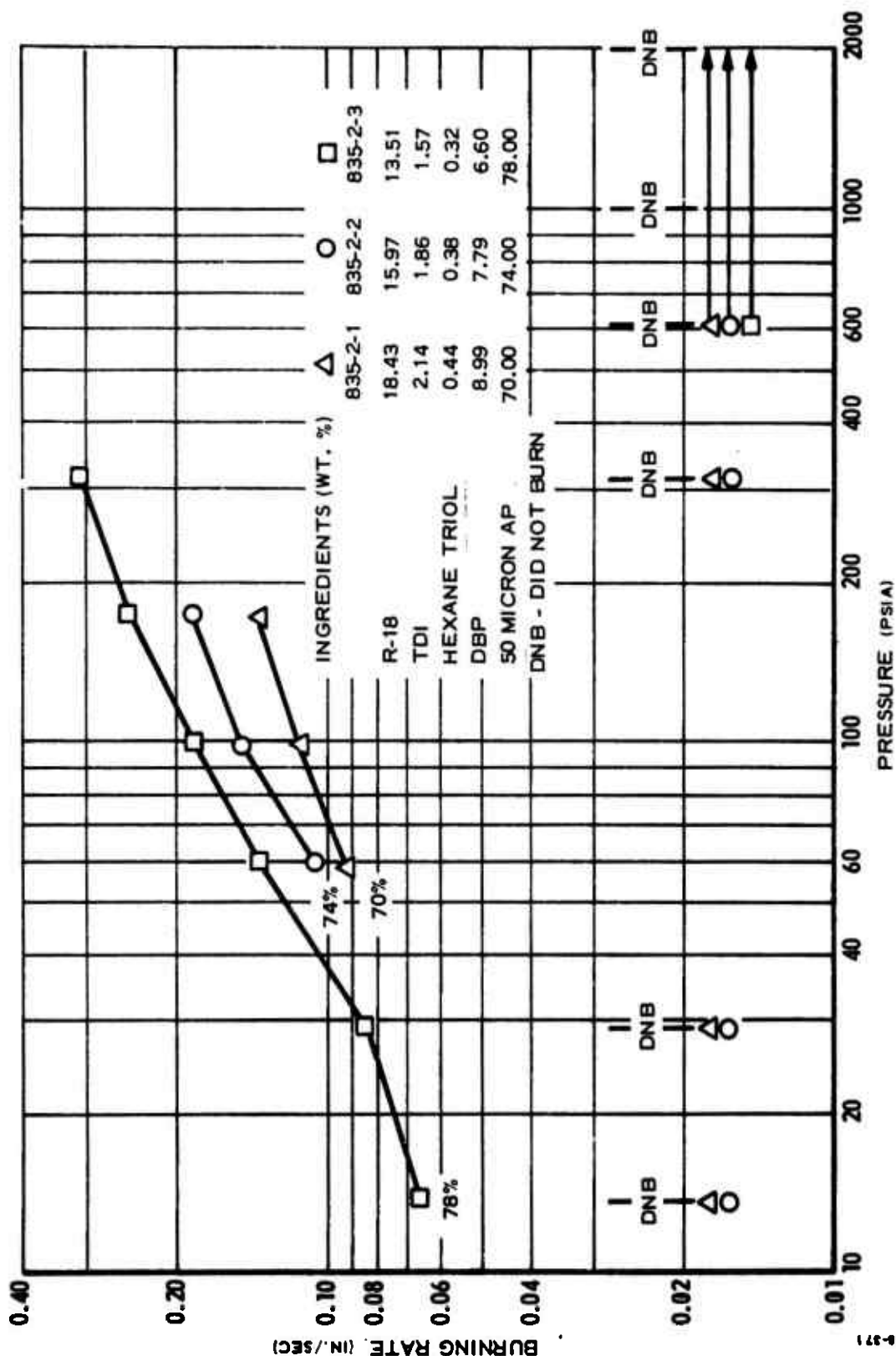


Figure 3 Burning Characteristics of Propellants Showing Effect of AP Level

CONFIDENTIAL

LOCKHEED PROPULSION COMPANY

UNCLASSIFIED

propellant system increased the burning rate over the pressure range considered. However, the shape or slope remains approximately unchanged over the pressure ranges where the propellants burned.

(U) It was found that combustion was not sustained in these propellants over the range of pressure at which burning rates were attempted (1 atmosphere to 2000 psia). It also was observed that the propellant containing the highest concentration of AP (835-2-3) burned over a greater pressure range than that of the other two propellants. This appears to indicate that a deficiency in the oxidizing species, at and above the surface at those pressures where the propellant will not sustain combustion, could lead to self extinguishment. In particular, self extinguishment could manifest from special sources:

- The rate of oxidizer decomposition is too slow and the oxidizer concentration too low to supply sufficient energy to sustain combustion at low pressures.
- The binder is melting, running over, and quenching decomposing oxidizer crystals at high pressure.
- The AP burning rate at high pressure is too rapid to maintain the required statistical geometric balance between AP and binder.

(U) Further discussion of these postulates describing self-extinguished samples is included under a later section of this report dealing with surface structure studies of extinguished propellants.

(U) Burning rates for three propellants having the same oxidizer concentration and changes in the oxidizer grind size are presented in Figure 4. The effect of increasing the particle size is seen to increase the burning rate. For the largest particle size (935-2-4), a slight decrease in slope was noted at pressures around 50 psia. Additional datum points were taken near 50 psia which verified the existence of this drop in slope. Further evidence that this is a real effect was revealed in the literature. Burning rate data for AP oxidized propellant with large particle sizes as reported (11) shows this same effect at pressures close to 50 psia.

(U) Self-extinguishment characteristic of these propellants provides new evidence that melting binder could be smothering the decomposing AP crystals at high pressures. Since the larger crystals project above the burning surface higher than the small crystals, it would be expected that the decomposition of larger crystals would not be as susceptible to quenching. In addition, the area of decomposition sites would be greater for the larger crystals than for the smaller crystals. Thus, the binder would have to flow over a greater area to smother the oxidizer decomposition process. On the other hand, those AP crystals depressed at higher pressure may be consumed before a succeeding layer is exposed.

(U) Although these formulations are not representative of useful propellants, and the self-extinguishment phenomena appear to be unique to

UNCLASSIFIED

**UNCLASSIFIED**

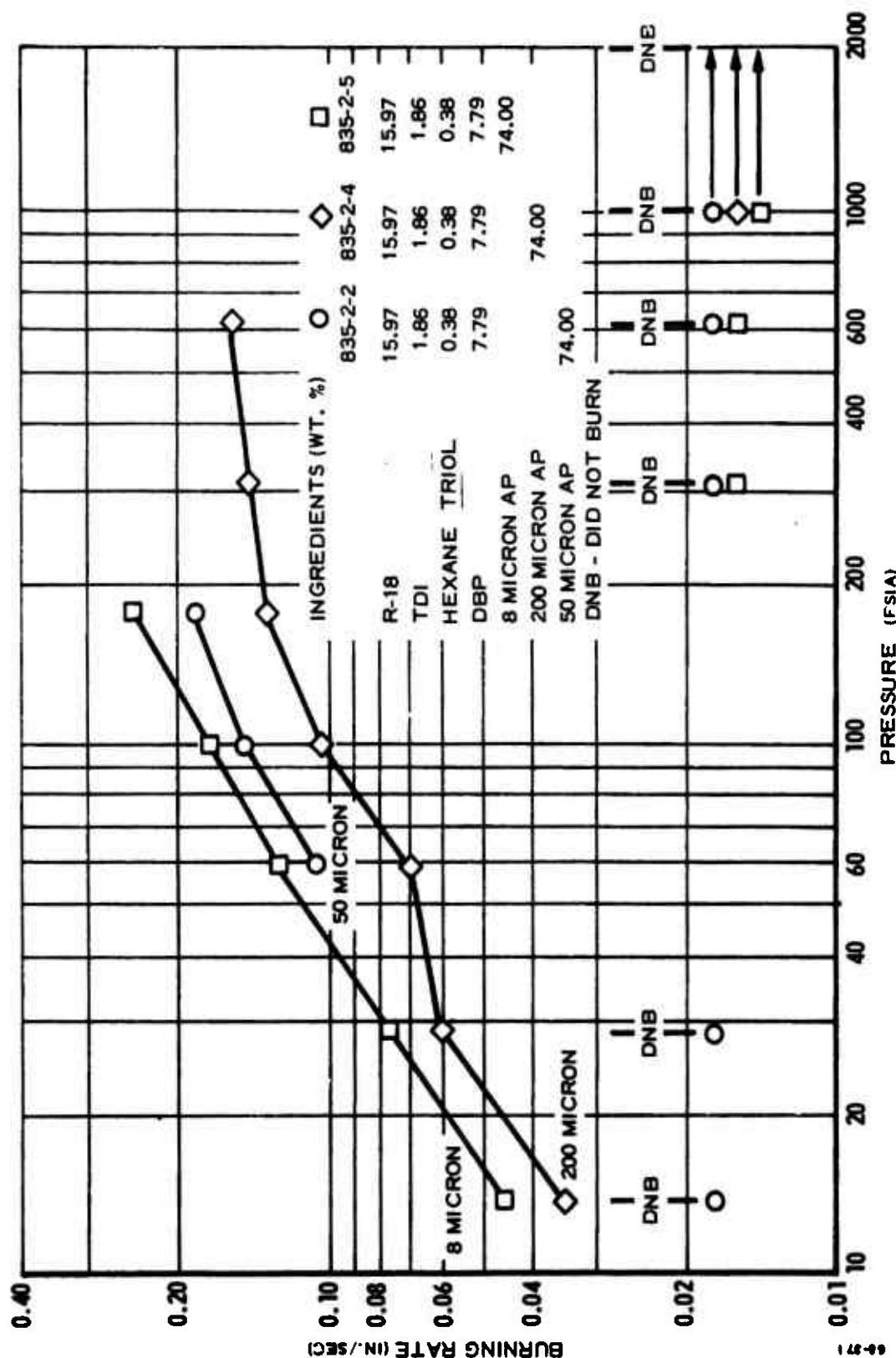


Figure 4 Burning Characteristics of Propellants Showing Effect of AP Size

**UNCLASSIFIED**

UNCLASSIFIED

propellants of this type, the data being obtained will be valuable for the combustion modeling of the non-metalized system and for determination of the role of metal in the modeling of a practical system.

### c. Propellants Containing KP

(U) Propellants oxidized with KP are of interest because they behave so differently from ammonium perchlorate propellants and because KP is not a monopropellant. In addition, the decomposition of KP does not produce an acid such as  $\text{HClO}_4$  which could lead to heterogeneous attack of the binder. Rather, it forms molten  $\text{KCl}$  and  $\text{O}_2$ . As a result, experimental studies using propellants containing KP should lead to information helpful in developing the CT model.

(U) Five propellant formulations were prepared containing KP as the oxidizer. These propellants had varying concentrations of oxidizer (viz. 70, 74, and 78 percent by weight) and three unimodal particle distributions (viz. 20, 50, and 100-micron mean diameter).

(U) Burning rates for three propellants having the same oxidizer size (50 microns) with changes in the KP concentration are presented in Figure 5. It can be seen that the effect of increasing KP concentration is to slightly increase the burning rate at pressures less than 1000 psia. At higher pressures, it appears that the burning rate is essentially the same for each of the selected formulations. Comparison of these data to burning rates measured for an arcite/KP propellant (12) show similar burning characteristics. Thus, these binders apparently do not play an important part in determining burning rate for propellants containing KP.

(U) Burning rates and formulations for two propellants showing the effect of KP grind size are shown in Figure 6. At low pressures, it appears that the finer grind KP yields higher burn rates than indicated for the coarse grind KP.

(U) However, at higher pressures (greater than 300 psia) the opposite trend is observed. Thus, it would appear that the effect of KP particle size is dependent upon pressure and cannot be generalized. A similar effect has been reported in the literature for KP/AP combinations wherein finely ground KP produced lower burning rates than coarse ground KP over pressures ranging from 60 to 1500 psia (13).

(U) The propellant formulation containing coarse ground KP (835-4-4) was not available for comparison purposes in this plot. When these data are obtained, the effect of varying KP size should be better understood.

(U) Self-extinguishment of the KP oxidized propellants was observed only at low pressures. The absence of extinguishment at the higher pressures could be a result of the decomposition processes of the KP. Perhaps the presence of molten KP on the surface could provide a basis for this difference to the previously described results for AP oxidized propellants.

UNCLASSIFIED

UNCLASSIFIED

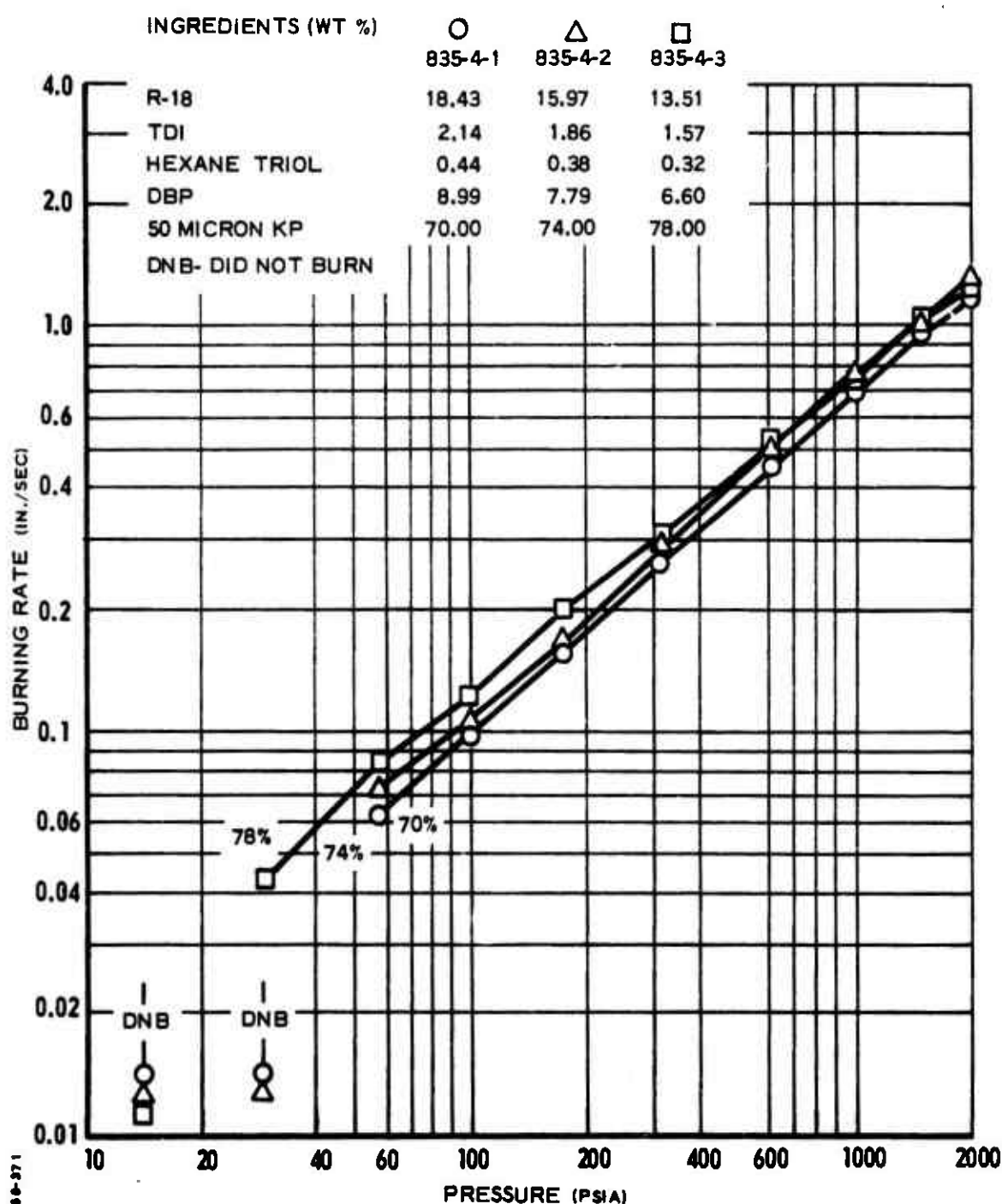


Figure 5 Burning Characteristics of Propellants Showing Effect of KP Level

UNCLASSIFIED

**CONFIDENTIAL**

(This page Unclassified)

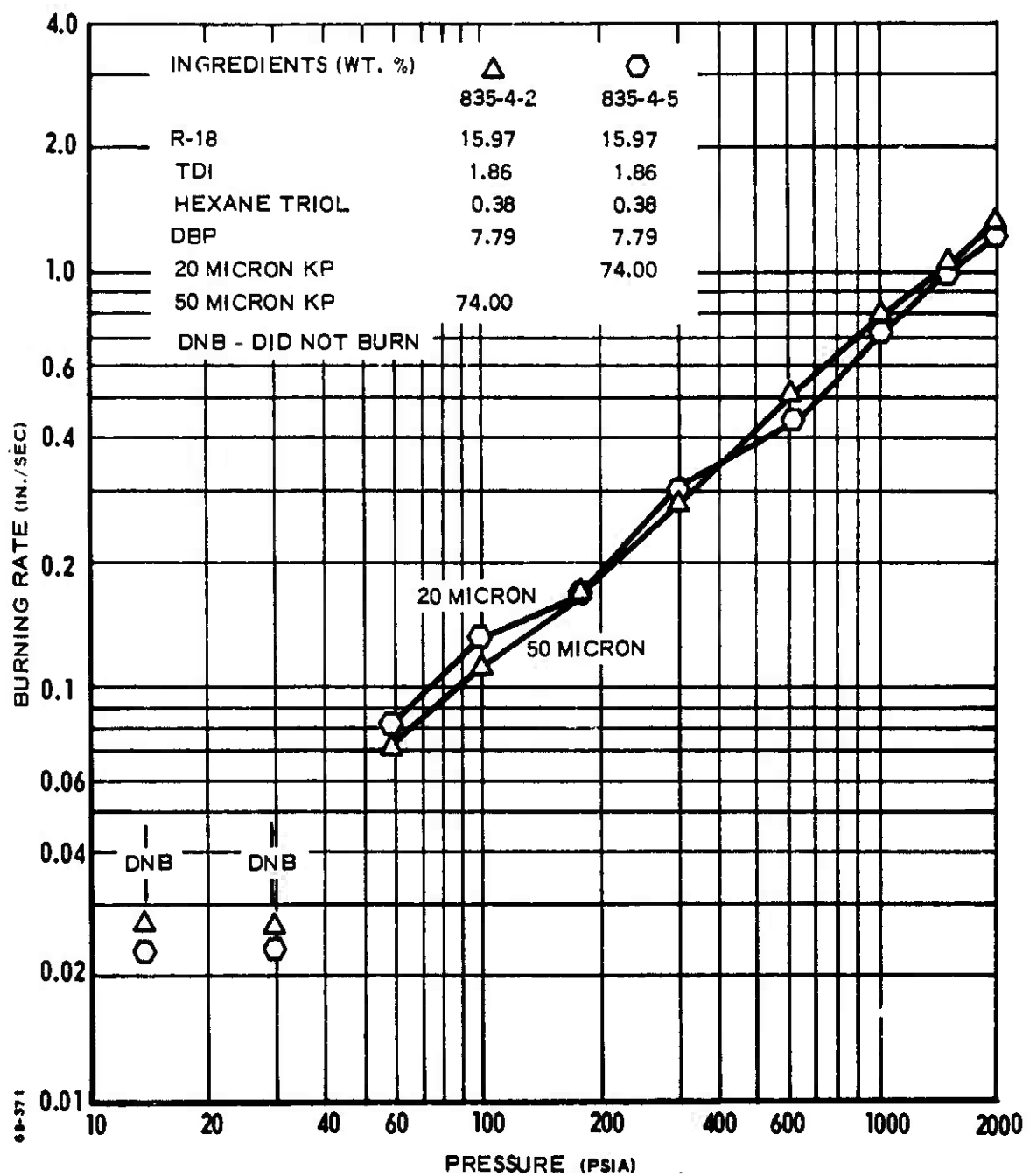


Figure 6 Burning Characteristics of Propellants Showing Effect of KP Size

**CONFIDENTIAL**

(U) At low pressures, the propellant containing the largest concentration of KP (835-4-3) burned where those containing lesser amounts would not sustain combustion. It appears here that the same reason as postulated for the AP oxidized propellants can be offered for this combustion limitation. The stoichiometry of the combustion process is too fuel rich to sustain combustion. Although KP liberates more oxygen than does AP, the existence of a molten layer of KCl could contribute to quenching at higher pressures.

(U) The fairly uniform high slope of the KP propellant system is suggestive of a second-order gas phase diffusion flame reaction as governing.

#### d. Propellants Containing HAP

(C) Propellants containing HAP are of interest to this research program because of their potential in supplying higher specific impulse than AP oxidized propellants. To allow development of the CT model to include this type of oxidizer, four formulations were prepared for experimental study. In these, the oxidizer concentration was maintained constant and the grind size varied over four particle distributions. Three of these particle sizes were obtained by screening a broad distribution of HAP to yield a relatively fine (45-105 micron), medium (105-210 micron), and coarse (greater than 210 micron) grinds. The fourth size consisted of the broad distribution unscreened (135-micron mean diameter).

(C) Burning rate for propellants containing HAP are presented in Figure 7. The particle size effect is somewhat similar to results presented for propellants containing KP. Propellants containing finer grind HAP burn faster than the coarse material at low pressures; while at high pressures (greater than 1200 psia), the opposite trend appears. It is interesting to note that such an effect was not found using AP propellants within the imposed pressure limits. However, the shape of the curves resembles that of AP propellants.

(C) Comparison of burning rates for the HAP with broad particle distribution (835-5-5) to those of the three relatively narrow cuts yields an interesting interdependence of the burning rate upon grind size. At low pressures, the broad distribution HAP showed rates close to the coarse material. However, at pressures above 400 psia, the rates of the broad distribution and fine material were approximately the same. Bastress found an opposite trend with bimodal AP systems (14).

(C) Therefore, while the character of the burning rate of the HAP system is similar to that of the AP system in some respects, there appears to be a subtle difference in particle size effects. A major difference is the ability of the HAP system to sustain combustion at higher pressures than could AP of equivalent particle size. Perhaps the HAP crystal does not burn as fast and become as depressed into the surface as does the AP crystal.

CONFIDENTIAL

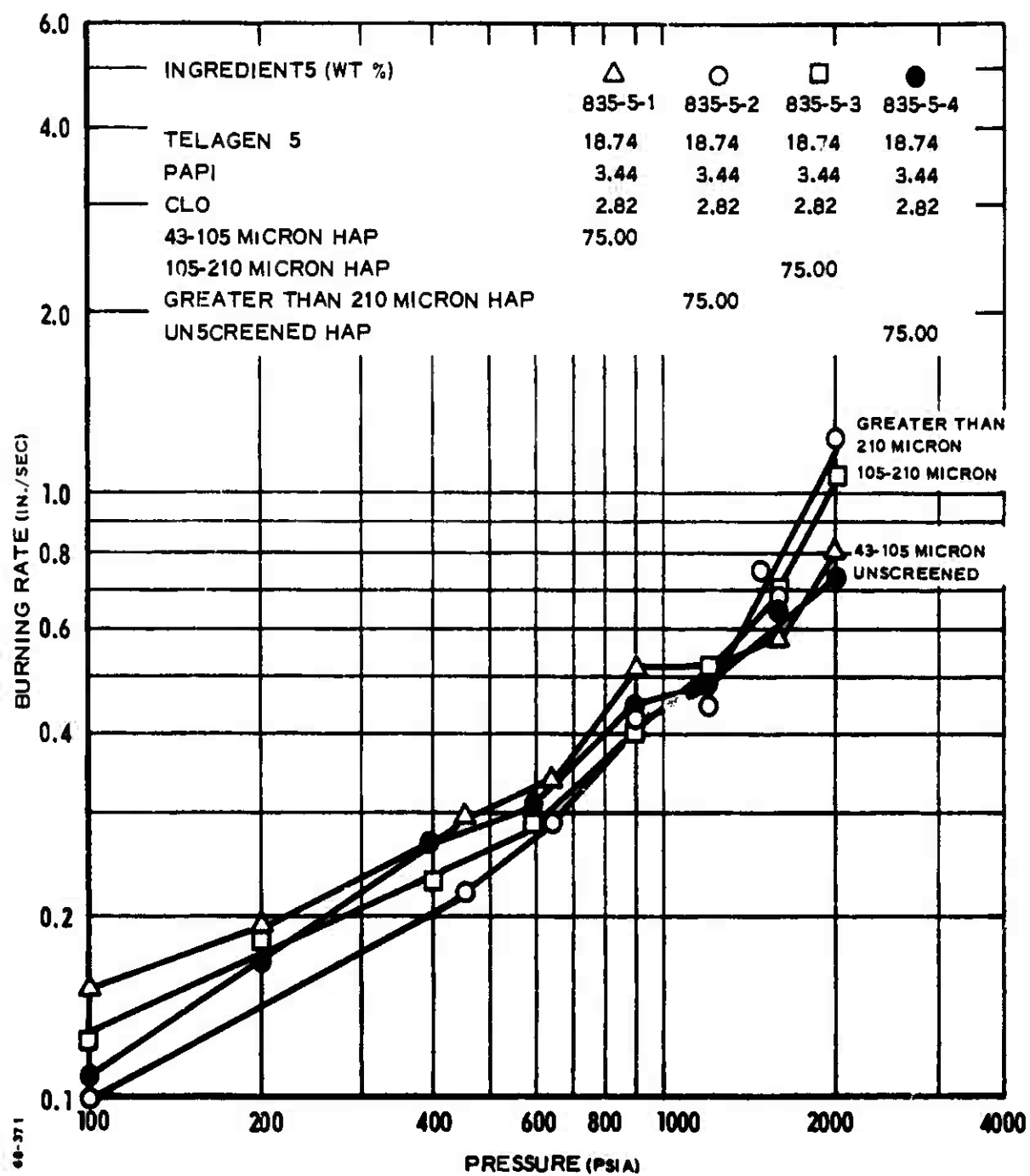


Figure 7 Burning Characteristics of Propellants Showing Effect of HAP Size

CONFIDENTIAL

## e. Propellants Containing HMX

(U) HMX is of interest in this research program because its combustion properties, when burned in a binder matrix, can be related to parametric changes in the CT model. Since HMX is a crystalline powder, it can be likened to AP, HAP, and KP in physical description. However, it is not an oxidizer *per se* because it burns as a monopropellant yielding products that contain negligibly small fractions of oxidizing species when compared to the previously mentioned oxidizers. Thus, experimental data from propellants containing HMX alone could provide data concerning changes in stoichiometry of the combustion process. Further parametric changes that HMX provides include a very high decomposition flame temperature compared to that of AP or HAP, and the possibility that heat transferred back to the binder surface is not controlled by diffusion of the binder pyrolysis products with oxidizing species.

(U) Five propellant formulations were prepared using HMX as the oxidizer. These propellants had varying concentration of HMX (viz. 70, 74, and 78 percent by weight) and three particle size distributions (viz. class A, class B, and class E).

(U) Burning rates for three propellants having the same HMX grind size (class B) with the above mentioned concentration changes are presented in Figure 8. Pressures below which combustion was not sustained were higher for these propellants than found for previously discussed propellants, possibly reflecting the poor stoichiometry. At pressures where combustion was sustained for all three HMX propellants, the concentration changes showed little influence upon the burning rate, and the character of the curve is similar to that with KP.

(U) Because of the small fraction of oxidizing species available to these propellant, it appears that the burning is controlled by the pressure-dependent heat transfers to the binder. Thus, the slow rates may be representative of binder thermal degradation.

(U) Burning rates for two propellants containing the same HMX concentration (74 percent by weight) and different particle distribution are presented in Figure 9. It can be seen that the propellant containing coarse HMX (835-6-4) has a lower burning rate than the propellant containing medium material (835-6-2). However, at high pressure, the coarse HMX propellant shows an increase in slope not found with the propellant containing medium material. Burning rates for a propellant containing a fine particle size of HMX have not been completed. These data will provide further information regarding the effect of HMX size on burning rate.

## (U) 3. STUDY OF THE SURFACE STRUCTURE OF EXTINGUISHED PROPELLANTS

The purpose of this study is to gain information concerning the physical nature of the burning surface of solid propellants. Results obtained from this study are used in incorporating realistic surface phenomena associated with the combustion process of different propellants in the CT model. The

UNCLASSIFIED

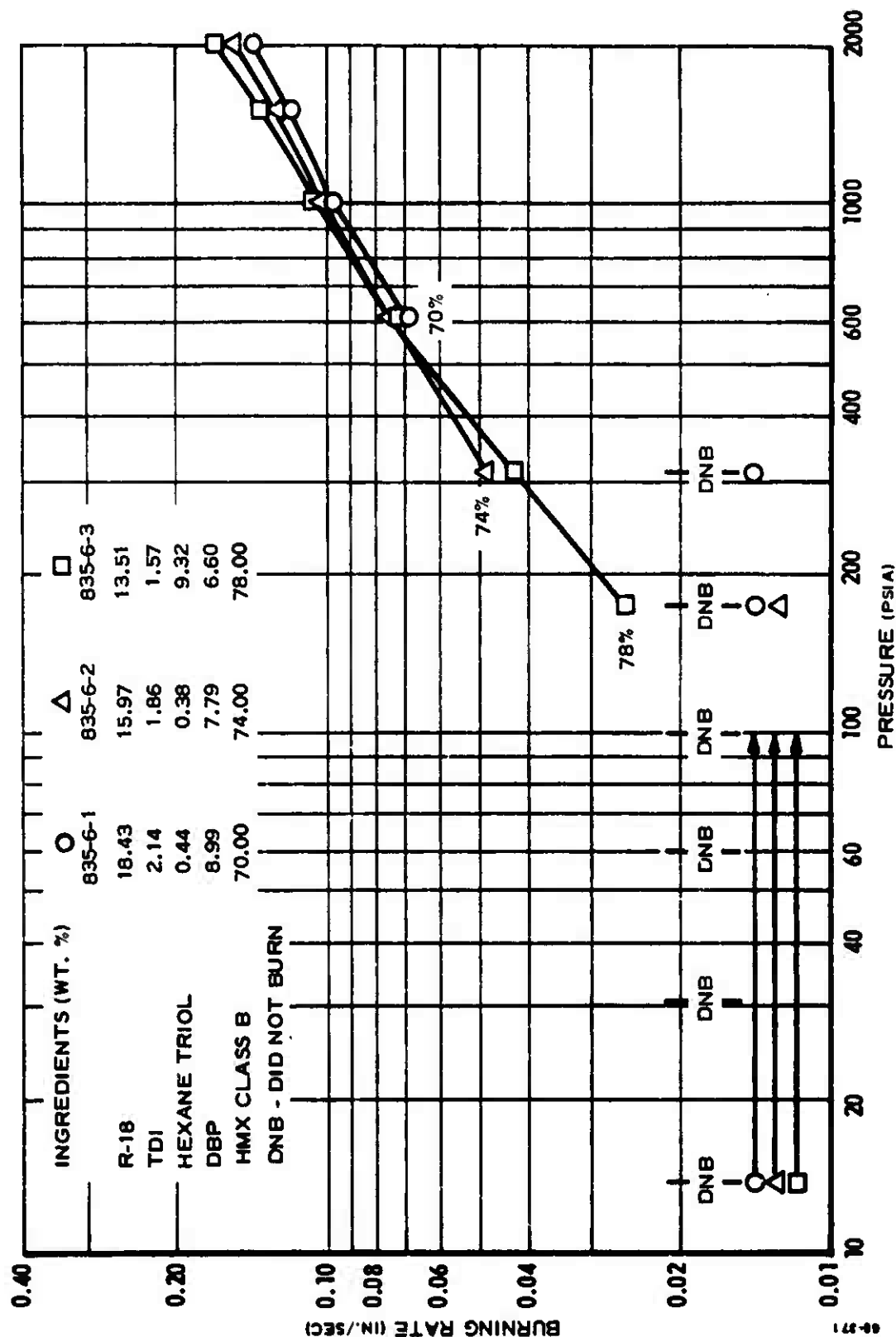


Figure 8 Burning Characteristics of Propellants Showing Effect of HMX Level

UNCLASSIFIED

UNCLASSIFIED

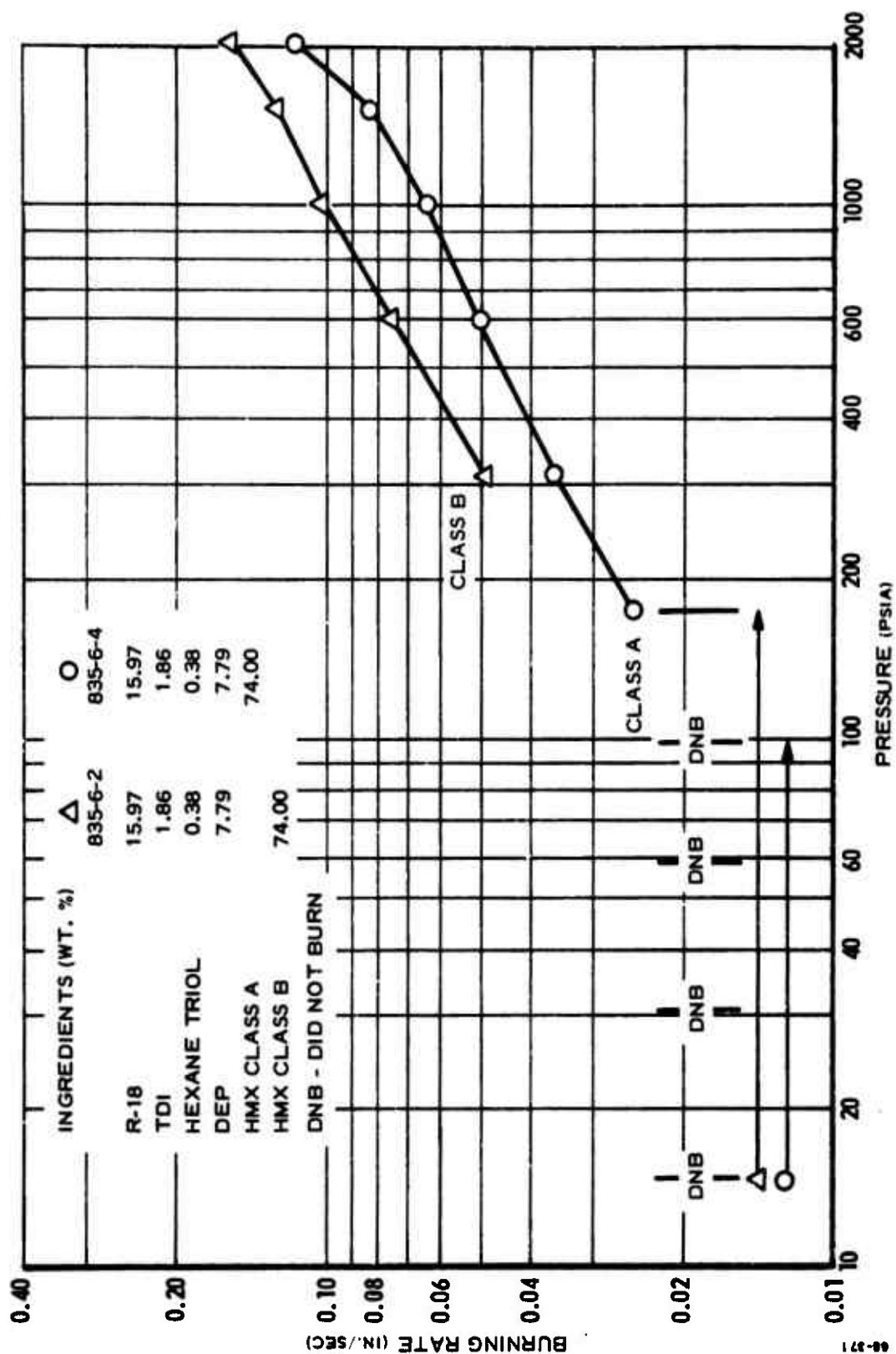


Figure 9 Burning Characteristics of Propellants Showing Effect of HMX Size

UNCLASSIFIED

approach followed is to extinguish burning samples of propellant in a combustion bomb by rapid depressurization and infer the structure of the burning surface from the observed structure of the extinguished surface. A description of the experimental apparatus is given in (5).

In the early stages of this experiment, extinguished samples of a CTPB/AP propellant were studied using an American Optical Microscope (Spencer Type Binocular Bench Scope) with 10-80X magnification. This method of examination was limited because of poor depth-of-field at higher magnification. The orientation of large crystals on the surface was discernible; however, inspection of surface microstructure (e. g., fine details on the surface of exposed crystals, fine details on the surface of the binder, and evidence of interaction along oxidizer binder interfaces) were not possible.

To remedy this limitation, an arrangement was made with Naval Weapons Center, China Lake, California, wherein Lockheed Propulsion Company would supply extinguished samples to NWC for the purpose of inspection through a scanning electron microscope (SEM). The SEM enables viewing of the samples at magnifications up to 100,000X (up to 2300X is used in this study) while retaining depth of fields far superior to the optical microscope. Analysis of photographs taken through the SEM was conducted jointly with NWC personnel.

Photographs are presented showing extinguished surfaces of propellants consisting of ammonium perchlorate and either a CTPB binder (referred to as Mod AGC-NOAL) or a PU binder (propellants 835-2-2 and 835-2-4). These photographs represent the first results obtained through a SEM in this research program for the purpose of surface structure studies. Because of this, observations reported herein should be considered of a preliminary nature until comparisons can be made to photographs obtained using other propellant systems.

Figures 10 and 11 present typical photographs taken through the SEM of samples consisting of 22-percent PU binder and 78-percent 50 micron ammonium perchlorate (835-2-2) which were burned at pressures of 100 psia, 200 psia, and 300 psia. Inspection of the photographs shown in Figure 10 reveals that, at low pressures, the pyrolysis rate of the AP was less than that of the binder, thus confirming the observation reported by Bastress (14) that the AP protrudes above the binder surface at low pressures. Also, the smooth flowing appearance of the binder suggests that the PU binder was molten during burning. It is of interest to note that all of the views shown in this figure indicate definite "undercutting" of the PU at the oxidizer particles' boundaries. Such an undercutting possibly could indicate that, at these low pressures, heterogeneous reactions as modeled by Hermance occurred between the AP and the binder during combustion. However, another possibility is that the diffusion flame between the decomposition products of the AP and the binder is so close to the surface at this low pressure that the heat transfer to the interface is enhanced causing the undercutting. At pressures of 200 and 300 psia, the AP crystals still appeared to protrude above the binder surface, as shown in Figure 11.

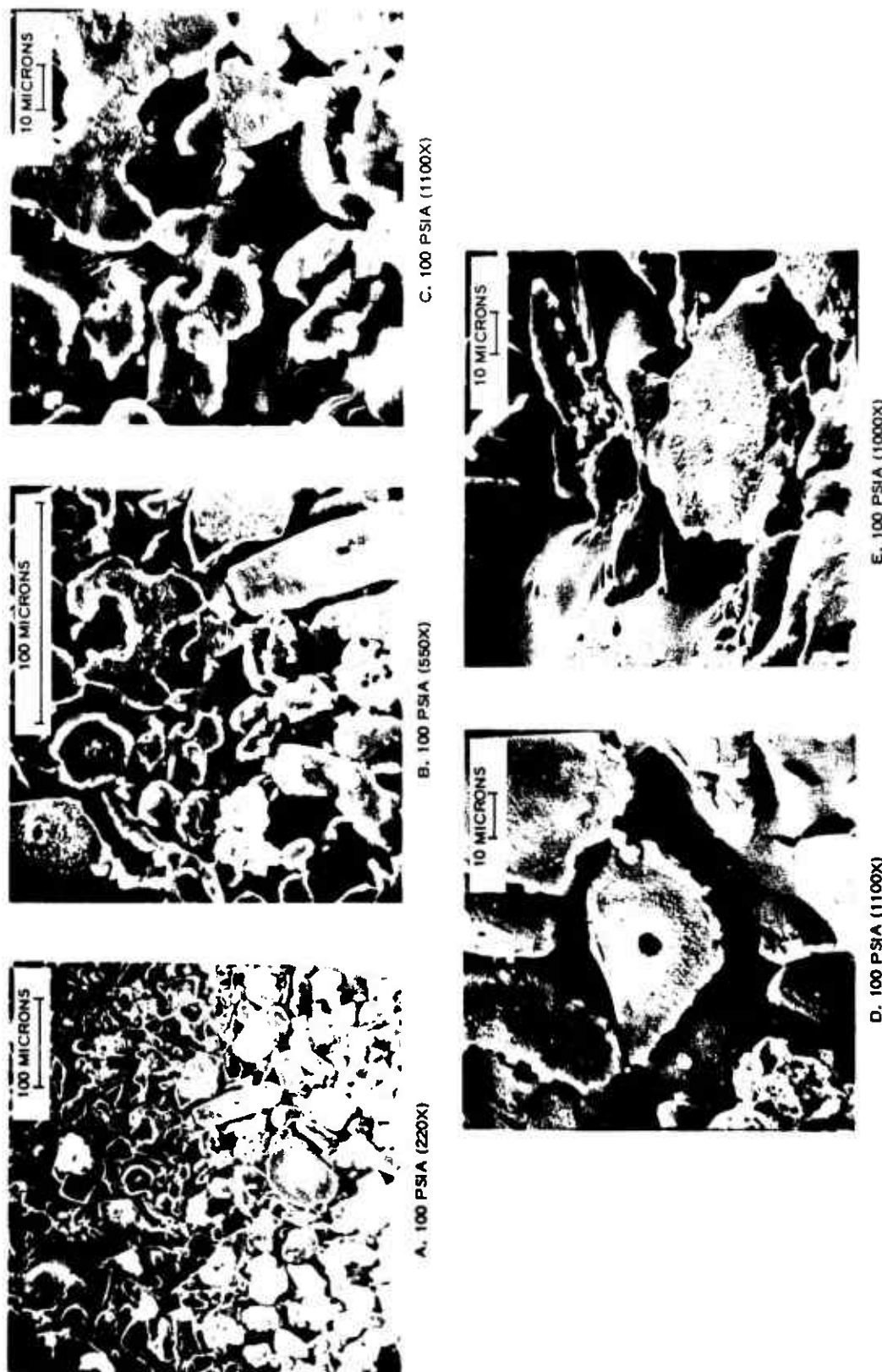


Figure 10 SEM Photographs of 835-2-2 at 100 psi

UNCLASSIFIED

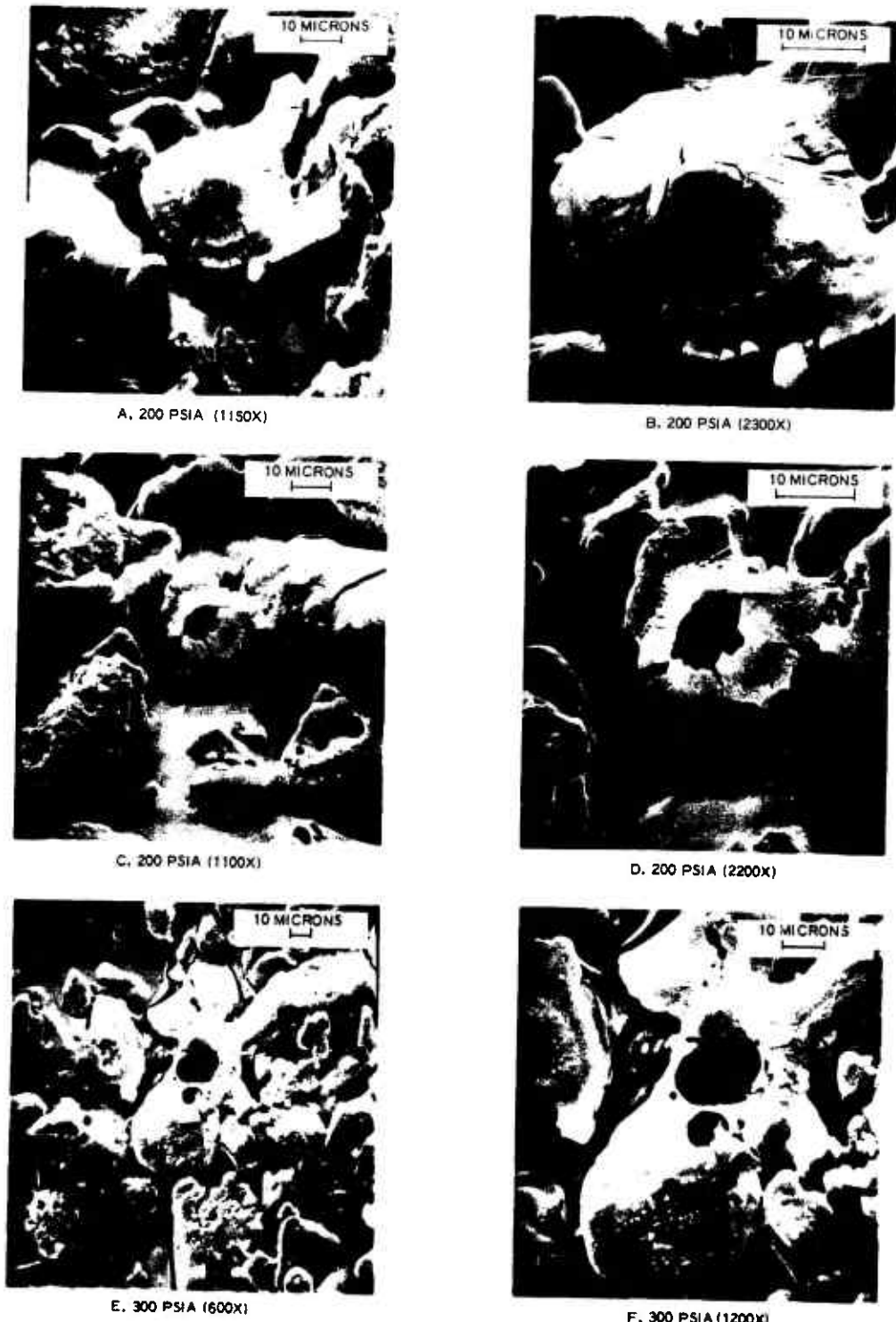


Figure 11 SEM Photographs of 835-2-2 at 200 and 300 psi

UNCLASSIFIED

Photographs of a propellant consisting of 26-percent PU binder and 74-percent 200 micron AP (835-2-4) are shown in Figure 12. These photographs illustrate the effects of pressure on the surface structure. The photographs on the left (Figures 12a, 12c, and 12e) are for samples extinguished at a pressure of 100 psia and those on the right were obtained at 800 psia. Both sets of samples dramatically indicate that the binder was molten prior to quench. At the lower pressure, the AP crystals protrude above the binder surface and undercutting is again noted. Whereas at the higher pressure, the AP crystals are recessed below the binder surface to the extent that the molten binder has apparently flowed into the recesses and covered the AP surfaces (possibly during extinguishment). This phenomenon could lead to an explanation of why some PU propellants do not sustain combustion at high pressures as reported earlier. As the pressure is increased, the regression rate of the AP eventually becomes greater than the binder regression and the molten binder then flows over the AP crystals inhibiting their combustion and causing extinguishment. At pressures intermediate between these two extremes, the propellant surface follows the trend that might be expected (i.e., the regression rates of the binder and oxidizer appear to be equal at approximately 600 psia).

Figure 13 contains photographs of propellant type 835-2-4 burned at 600 psi. The bubble formation is typical of structures that have been observed in studies of AP deflagration using single crystals (7 and 15) and has been interpreted as indicating that the surface of the AP is covered by a thin molten AP layer. Gases formed from the decomposition of the AP within the molten layer expand during rapid depressurization causing the bubble formation as the AP freezes. Indeed, it would be difficult to explain the bubble-like structure without assuming the existence of a liquid state. Similar types of structures are evident in the majority of AP-oxidized samples studied. The volcano-like-structure seen in Figures 10d, 11c, and 11d, and the vented structures shown in Figures 11a and 11b, also appear to indicate condensed phase subsurface reactions taking place within the AP prior to quench. Furthermore, it appears that these reactions always occur in the portion of the AP crystal that indicates a molten state prior to quench. These structures and the microstructures observed in other photographs of these samples are typical of structures observed of AP samples heated by external sources at low pressures (15).

By mechanically stressing the quenched samples it was possible to break the AP/binder bond releasing the AP crystals as seen in Figure 14. Examination of the displaced crystals and one of the craters left undisturbed in the binder, as seen in Figures 14b and 14c, shows no indication of subsurface interfacial reaction between the AP and the binder.

The effect of binder-type on the surface structure was explored through SEM photographs of a propellant containing a CTPB binder. The propellant was examined previously through an optical microscope and reported in (5). Results from these tests at 600 psia are included in Figure 15. Figures 15a and 15b again indicate that the surface of the AP crystals were molten as with the PU binder and that subsurface reactions in the molten phase of the AP resulted in gas liberation within the molten phase. The photographs seen in Figures 15c-15e seems to indicate that interfacial

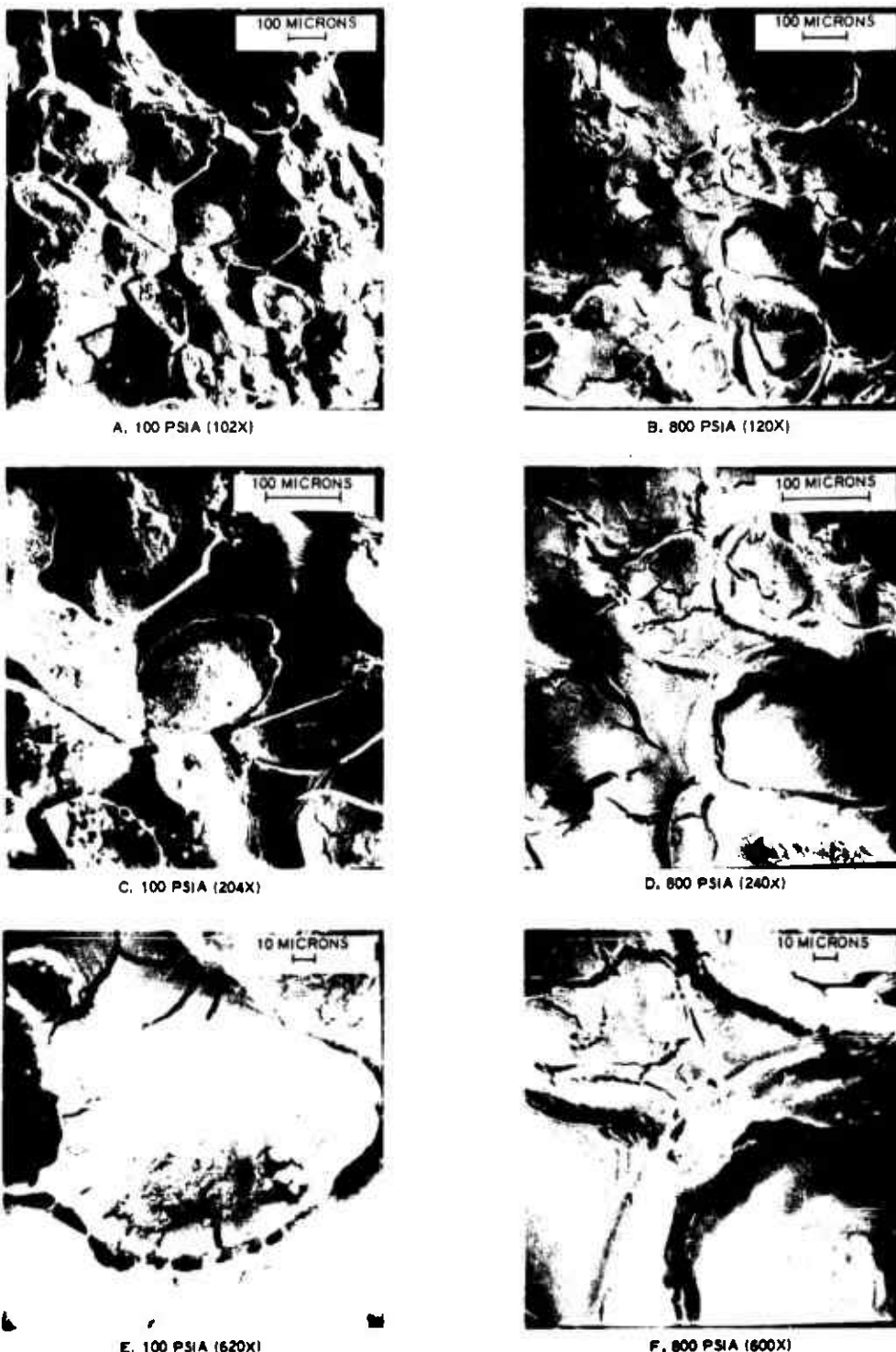


Figure 1.2 SEM Photographs of 835-2-4 at 100 and 800 psi



Figure 13 SEM Photographs of 835-2-4 at 600 psi

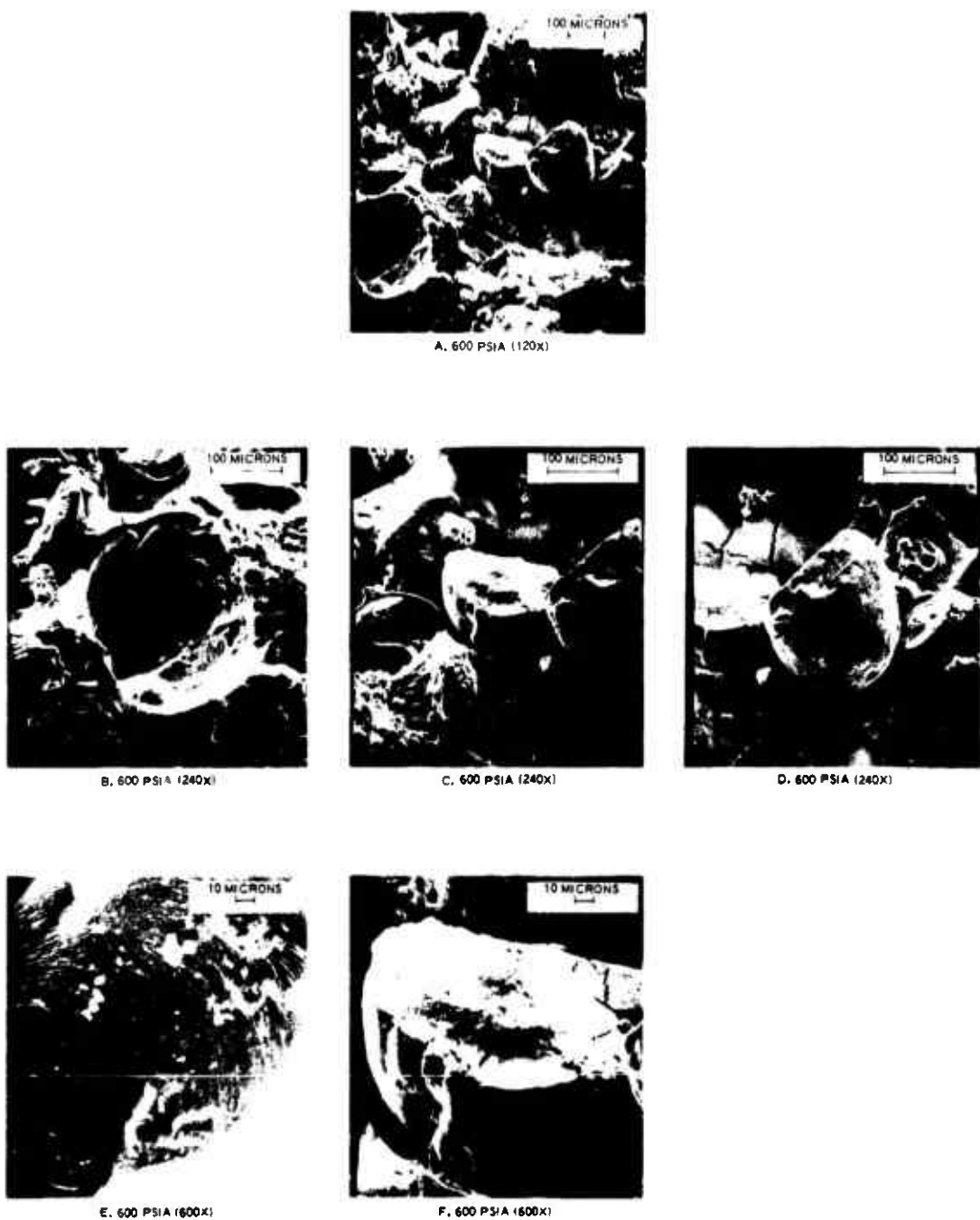


Figure 14 SEM Photographs of 835-2-4 at 600 psi Showing Crystal Detail

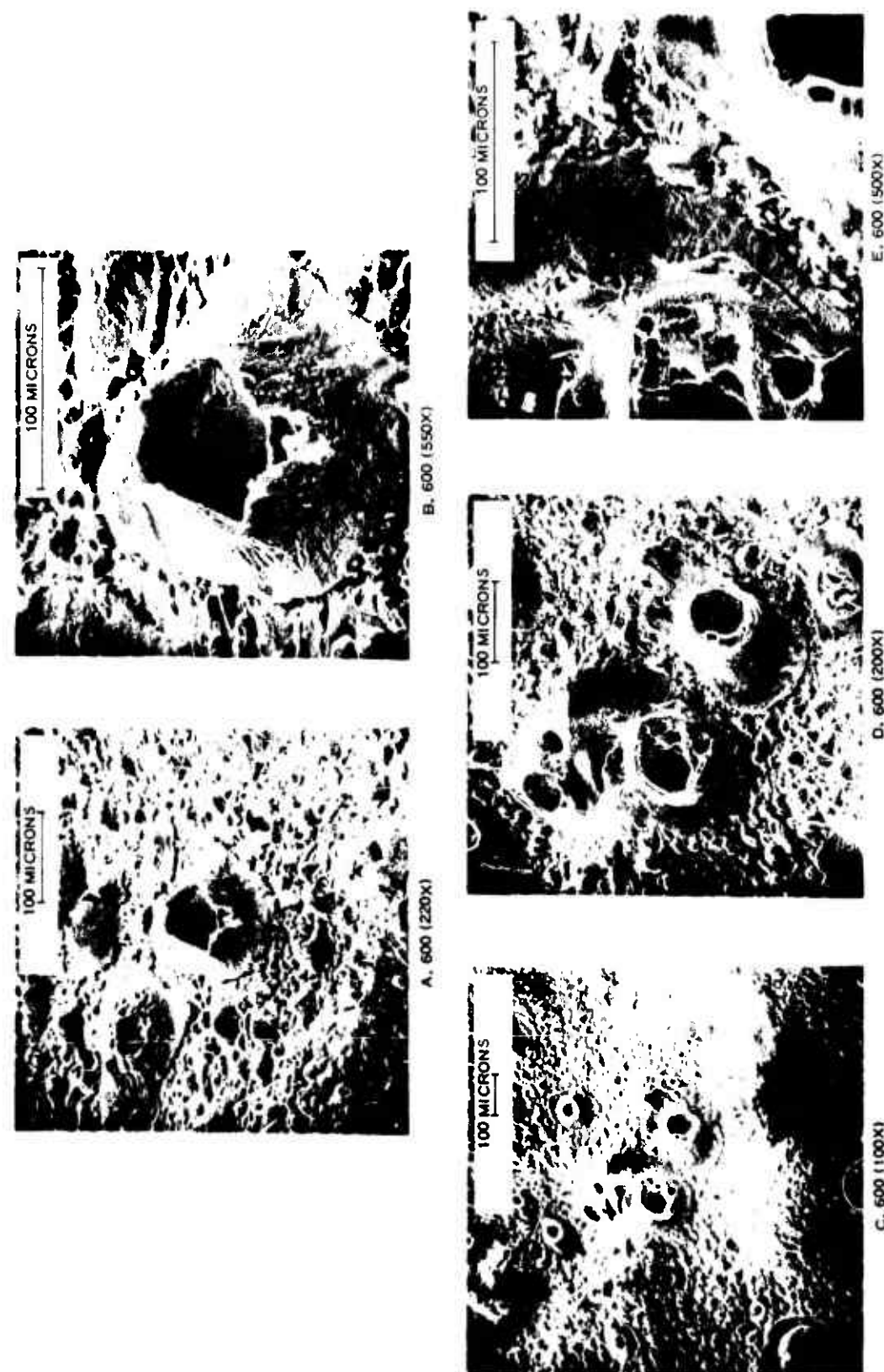


Figure 15 SEM Photographs of Mod AGC-NOAL at 600 psi

reactions were not present at the CTPB-AP interface at this pressure. In addition, the absence of undercutting at lower pressures seems to indicate a total lack of heterogeneous reactions at the AP/binder interface with the CTPB samples. Also, there is no indication of the CTPB binder melting as with the PU binder (i. e., the binder does not have a smooth flowing appearance nor the "cracked-mud" appearance as seen in Figure 12). An additional contrast in behavior between PU and CTPB propellants is that, at 600 psia, the AP crystals still protrude slightly above the CTPB binder. The CTPB binder may, therefore, have a higher pyrolysis rate.

A characteristically domed appearance of the AP crystals is demonstrated clearly in Figures 16a-16c for the PU/AP propellant which was burned at 528 psia. AP crystals released from the CTPB binder by mechanically stressing the quenched sample is shown in Figure 16d. Again, as observed with the PU propellants, the photography shows no indication of subsurface interfacial reactions between the AP and the binder.

The results presented above summarize only the more significant observations derived from SEM photographs of available AP oxidized propellants. Future studies of other propellants (as outlined earlier) could possibly expose some phenomena not immediately recognizable in the photographs presently available.

#### (U) 4. THERMAL PROFILE STUDIES USING MICROTHERMOCOUPLES

The objective of this study is to measure the thermal profile in propellants by embedding fine chromel-alumel wire thermocouples (0.0003 in. diameter) in propellant samples. The thermal profile beneath the propellant surface is dependent upon the burning rate, thermal wave characteristic time, surface temperature, and heat release within the solid. Information can be derived from a thermal profile by examining the change in the slope of that profile. Small changes in the slope can indicate the presence of exothermic or endothermic reactions within the solid. Whereas, abrupt changes in the slope can indicate the thermocouple has reached the surface; thus, the surface temperature can be found. A detailed discussion of data analysis techniques for thermal profiles is presented in (4).

Thermal profiles were measured in propellants containing 26-percent PU binder and 74-percent class A HMX (propellant 835-6-4) at pressures of 200, 300, and 400 psia. The results of these tests, shown in Figures 17 through 19, indicate that the surface temperature of the PU/HMX propellant is about 780°C. In every case, the temperature profile slope changed abruptly at this temperature. Additional thermal profiles at 200 and 300 psia confirmed this temperature.

The overall shape of each of the thermal profiles indicate that the propellant was preheated to a depth exceeding a distance expected from thermal conduction alone. This "in depth" heating was discussed in a previous report (4) and was attributed to radiative preheating of the solid. Small changes in the thermal profile slope could be due to exothermic or endothermic reactions within the solid. To check this hypothesis, samples

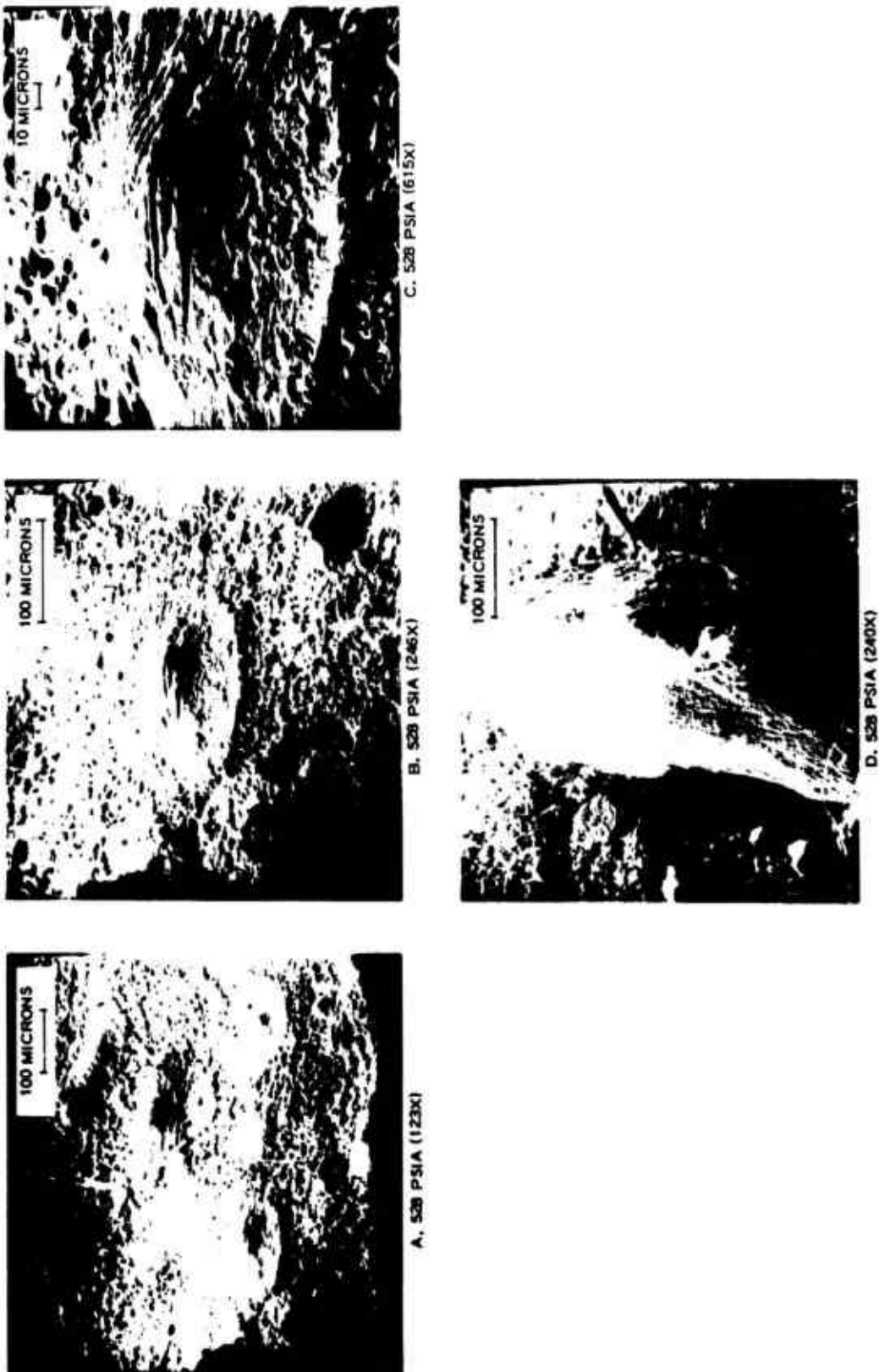


Figure 16 SEM Photographs of Mod AGC-NOAL at 528 psi

UNCLASSIFIED

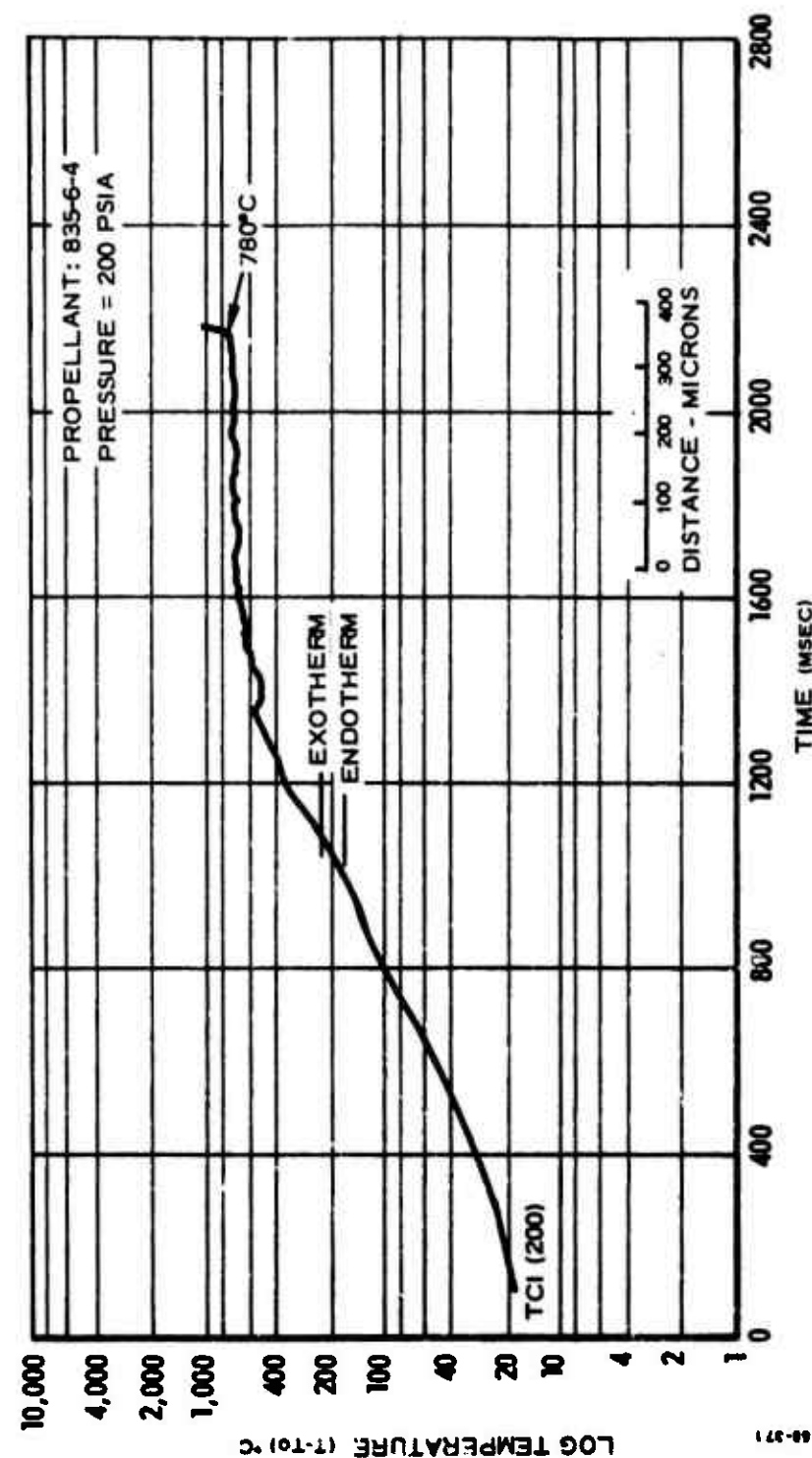


Figure 17 Thermal Profile of 835-6-4 at 200 psia

UNCLASSIFIED

UNCLASSIFIED

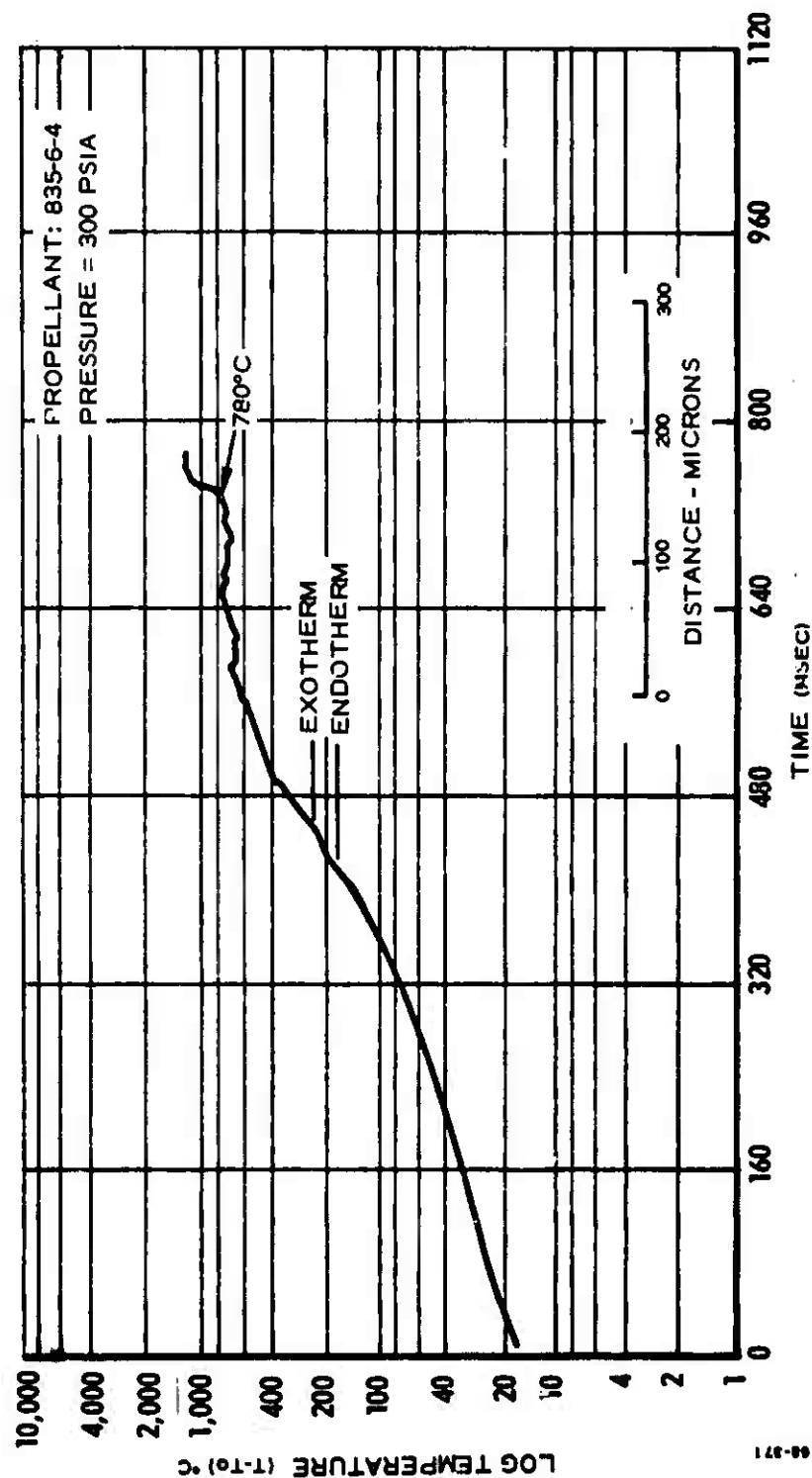


Figure 18 Thermal Profile of 835-6-4 at 300 psia

UNCLASSIFIED

UNCLASSIFIED

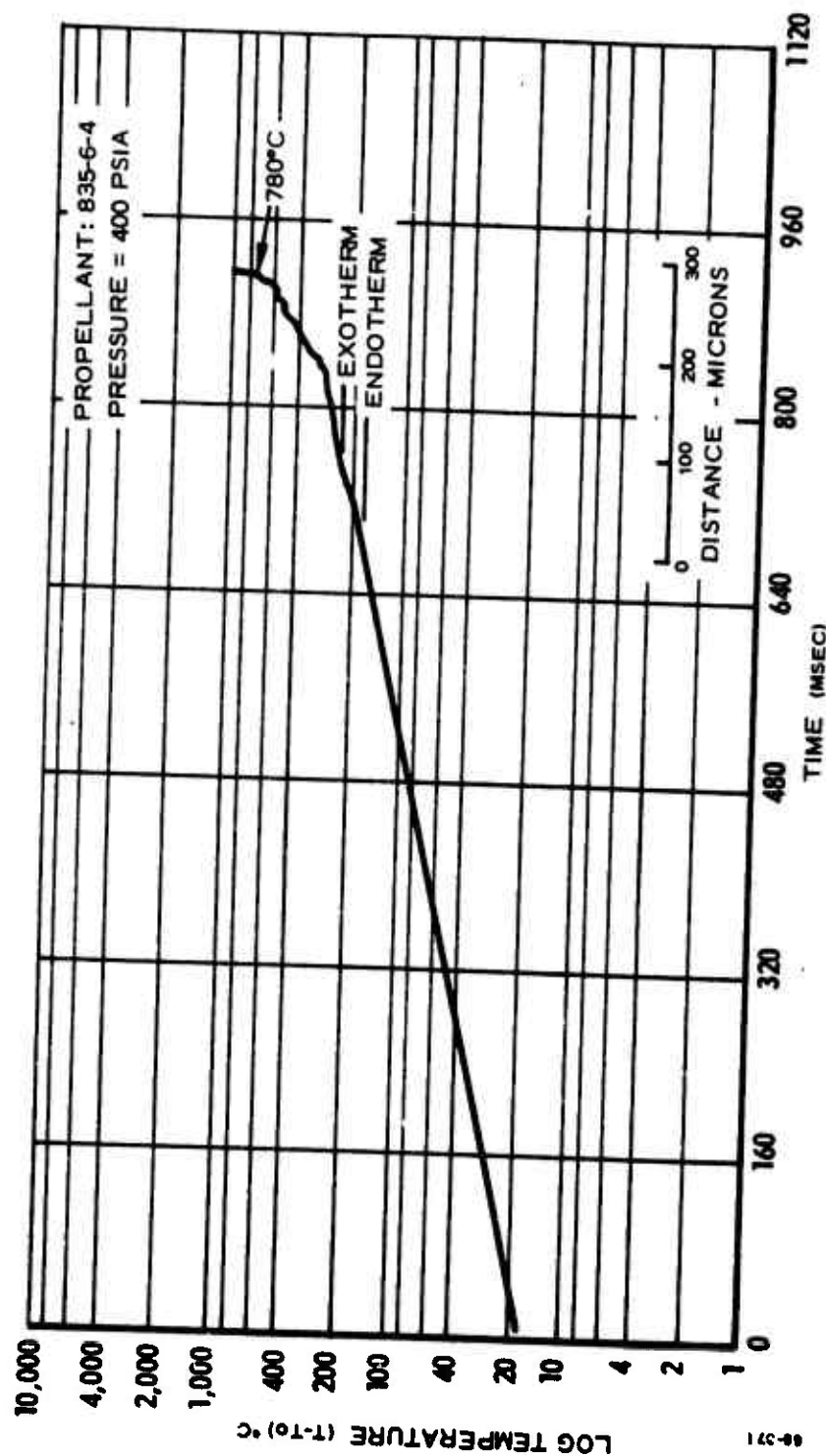


Figure 19 Thermal Profile of 835-6-4 at 400 psia

UNCLASSIFIED

**UNCLASSIFIED**

of the same propellant were tested on a differential scanning calorimeter (DSC). Results showed that this propellant has a small endotherm beginning at 200°C that reaches a peak at 204°C. Following the endotherm, the propellant exhibits a large exotherm beginning at 247-257°C and reaches a peak at 297-305°C. The peak temperature of the endotherm and exotherm are shown in Figures 17 through 19 for comparison purposes to the thermal profile results. In every case, the change in the thermal profile is as would be expected. The slope increases for an endotherm and decreases for an exotherm.

These data appear encouraging in that they show a definite trend when compared with previous thermal profiles measured in the research programs with AP. The DSC results have, in general, correlated with the thermal profile shape. Although surface temperatures could not be accurately measured from profiles obtained for propellants containing AP, results for propellants containing HMX are consistent and allow accurate measurement of the surface temperature. Future studies using other propellants will provide further information that can lead to better analysis techniques of the thermal profiles.

**UNCLASSIFIED**

**CONFIDENTIAL**

## SECTION V

## PLANS FOR THE NEXT PHASE

## 1. ANALYTICAL INVESTIGATION

(U) The equations describing the two-stage flame structure will be incorporated into the overall model and programmed for the computer. The various parameters will be evaluated wherever possible by using realistic literature values. Where information is lacking in the literature, the optimization program that has been used in the past will be employed to arrive at a realistic correlation with experimental data.

(U) Once programmed, the model will be used to compare the computed burning rate trends with the burning rate data that is being gathered. This will permit an evaluation of the validity of the proposed model.

## 2. EXPERIMENTAL INVESTIGATION

(C) Testing of propellants having different oxidizers will be completed. Thermal profiles, high speed cinematography, and surface structure studies will be conducted for each of these propellants. In addition, burning rates will be measured for a reference control propellant (835-8-1) containing saturated hydrocarbon/AP. Testing with this propellant is necessary because of the required change in binder for the HAP oxidized propellants (see Table I).

(U) Preparation of propellants containing metals and active binders will be completed in the next quarter. Testing of these propellants will be initiated using windowed apparatus and the slab combustor.

(The reverse is blank)

**CONFIDENTIAL**

**CONFIDENTIAL**  
(This page Unclassified)**NOMENCLATURE**

A	Arrhenius frequency factor
AP	Ammonium perchlorate
A, B	Constants in Equation (5)
b	Burner radius from Burke-Schumann analysis
c	Heat capacity
$\bar{c}$	Average mean heat capacity for the solid and gases
$c_g$	Heat capacity of the gases
CLO	Circo light oil
CTPB	Carboxy-terminated polybutadiene
D	Diffusion coefficient
$D_o$	Diffusion coefficient at reference point
DBP	Dibutyl phthalate
DNB	Did not burn
DSC	Differential scanning calorimeter
HAP	Hydroxylammonium perchlorate
HMX	Cyclotetramethylenetrinitramine
KP	Potassium perchlorate
m	Mass flux associated with propellant components
$m_T$	Total mass flux of propellant
M	Molecular weight
PAPI	A polyfunctional isocyanate (Carwin Division, Upjohn Co.)
PU	Polyurethane
Q	Heat release associated with combustion steps
$Q_L$	Latent heat of sublimation of AP

**CONFIDENTIAL**

**CONFIDENTIAL**

R	Gas constant
R-18	Multron, a hydroxy-terminated polyethylene glycol adipate (Mobay Chemicals)
r	Linear propellant burning rate
S	Surface area
S <sub>0</sub>	Total surface area
SEM	Scanning electron microscope
T	Temperature
TDI	Toluene diisocyanate
TVOPA	1,2,3-tris (1,2-bis(difluoramino)ethoxy)propane
v <sub>g</sub>	Gas velocity
x	Distance
x*	Flame standoff distance
a <sub>t</sub>	Thermal diffusivity
a	Weight fraction oxidizer
ΔH <sub>p</sub>	Heat of pyrolysis of binder
η <sub>av</sub>	Averaged non-dimensional distance determined from the Burke-Schumann analysis
λ	Thermal conductivity
λ <sub>g</sub>	Thermal conductivity of the combustion gases
ξ	Non-dimensional distance; $\frac{r}{a} x$
ξ*	Non-dimensional standoff distance
τ	Average gas phase reaction time

**Subscripts**

b	Refers to binder
ox	Refers to oxidizer
hr	Refers to heterogeneous reaction
f	Refers to final flame conditions
AP	Refers to AP flame conditions
p	Refers to solid propellant

**CONFIDENTIAL**

## REFERENCES

1. Hermance, C. E., "A Model of Composite Propellant Combustion including Surface Heterogeneity and Heat Generation," AIAA J., Vol. 4, No. 9, Sep 1966, pp. 1629-1637
2. Hermance, C. E., "A Detailed Model of the Combustion of Composite Solid Propellants," Proceedings of the ICRPG/AIAA 2nd Solid Propulsion Conference, Anaheim, California, 6-8 Jun 1967, pp. 89-103
3. Lockheed Propulsion Company, Solid Propellant Combustion Literature Review (U), Special Report No. 835-S-1 on Contract F04611-67-C-0089, Redlands, California, May 1968, (C)
4. Lockheed Propulsion Company, Combustion Tailoring Criteria for Solid Propellants, Phase II Report on Contract F04611-67-C-0089, Redlands, California, Apr 1968
5. Lockheed Propulsion Company, Combustion Tailoring Criteria for Solid Propellants, Phase III Report on Contract F04611-67-C-0089, Redlands, California, Jul 1968
6. Schultz, R. D. and A. O. Dekker, "Transition-State Theory of the Linear Rate of Decomposition of Ammonium Perchlorate," Sixth Symposium (International) on Combustion, Reinhold, New York, 1957, pp. 618-626
7. Hightower, J. D. and E. W. Price, "Combustion of Ammonium Perchlorate," Eleventh Symposium (International) on Combustion, The Combustion Institute, Pittsburgh, Pennsylvania, 1967, pp. 463-472
8. Burke, S. P. and T. E. W. Schumann, "Diffusion Flames," Ind. Eng. Chem., Vol. 20, 1928, p. 998 (see also, First and Second Symposium on Combustion, The Combustion Institute, Pittsburgh, Pennsylvania, 1965, pp. 2-11)
9. Penner, S. S., Chemistry Problems in Jet Propulsion, Pergamon Press, Los Angeles, 1957, p. 246
10. Inami, S. H., W. A. Rosser, and H. Wise, "Dissociation Pressure of Ammonium Perchlorate," J. of Physical Chemistry, Vol. 67, May 1963, pp. 1077-1079
- ii. Steinz, J. A., P. L. Stang, and Summerfield, "The Burning Mechanism of Ammonium Perchlorate-Based Composite Propellants," AIAA Preprint No. 68-658 presented at the AIAA 4th Propulsion Joint Specialist Conference, Cleveland, Ohio, June 1968

12. Friedman, R., J.B. Levy, and R.E. Rumbel, "Factors Governing Burning Characteristics of Composite Solid Propellants," Bulletin of the Fifteenth JANAF Solid Propellant Group Meeting (Washington, D.C., June 1959) Vol. IV, pp. 97-125
13. Lockheed Propulsion Company, "Study of Fluid Controlled Solid Propellant Rocket Motors (Restartable Solid Variable Pulse (RSVP) Motor) (U)," Final Report No. 734-F, Redlands, California, Aug 1967, (C)
14. Bastress, E.K., "Modification of the Burning Rates of Ammonium Perchlorate Solid Propellants by Particle Size Control," Ph. D. Thesis, Department of Aeronautical Engineering, Princeton University, Jan 1961.
15. Private communication with Mr. T. Boggs, Naval Weapons Center, Sep 1968.

DOCUMENT CONTROL DATA - R & D		
(Security classification of title, body of abstract and indexing annotation must be entered when the overall report is classified)		
1. ORIGINATING ACTIVITY (Corporate author) Lockheed Propulsion Company A Division of Lockheed Aircraft Corporation P.O. Box 111, Redlands, California		2a. REPORT SECURITY CLASSIFICATION CONFIDENTIAL-NOFORN
3. REPORT TITLE Combustion Tailoring Criteria for Solid Propellants		2b. GROUP 4
4. DESCRIPTIVE NOTES (Type of report and inclusive dates) Phase IV Report, Covering period 1 July to 1 October 1968		
5. AUTHOR(S) (First name, middle initial, last name) Ronald L. Derr and Merrill W. Beckstead		
6. REPORT DATE October 1968	7a. TOTAL NO. OF PAGES 50	7b. NO. OF REFS 15
8a. CONTRACT OR GRANT NO. F04611-67-C-0089	9a. ORIGINATOR'S REPORT NUMBER(S) LPC Report No. 835 Phase IV	
b. PROJECT NO. c. d.	9b. OTHER REPORT NO(S) (Any other numbers that may be assigned this report)	
10. DISTRIBUTION STATEMENT Qualified requestors may obtain copies of this report from DDC.		
11. SUPPLEMENTARY NOTES	12. SPONSORING MILITARY ACTIVITY Air Force Rocket Propulsion Laboratory Research and Technology Division Air Force Systems Command United States Air Force, Edwards, Calif.	
13. ABSTRACT The objective of this research program is to develop an analytical model describing the steady-state combustion of solid propellants which is suitably equipped to provide combustion tailoring criteria for both state-of-the-art and advanced propellant formulations. The model will be developed and implemented from experimental data acquired from a dual experimental program. Tests with small samples of propellants will provide experimental data for modeling the propellant combustion process for different ingredient variations, e.g., oxidizer size, concentration, and metals. Additional tests in apparatus simulating the environment of a rocket motor will provide experimental data showing the effect of rocket motor environment upon the combustion process. During Phase IV, analytical work was directed towards modeling the gaseous reaction zones above the surface of an ammonium perchlorate oxidized propellant. Experimental work was directed towards testing a series of propellants containing four different oxidizers.		

14. KEY WORDS	LINK A		LINK B		LINK C	
	ROLE	WT	ROLE	WT	ROLE	WT
Solid state combustion						
Steady-state combustion						
Solid propellant measurements						
Combustion kinetics						
Combustion tailoring						

# GENERAL DECLASSIFICATION SCHEDULE

IN ACCORDANCE WITH  
NIP 0309.13 & EXECUTIVE ORDER 13526

END

DATE

FILMED

12 68